MAGNETIC BEADS FOR CADMIUM REMOVAL FROM HUMAN PLASMA IN MAGNETICALLY STABILIZED FLUIZED BED (MSFB)

A Thesis Submitted to the
Graduate School of Natural and Applied Sciences of
Dokuz Eylül University
In Partial Fulfillment of the Requirements for
The Degree of Doctor of Philosophy in Chemistry Program

by
Nilgün YÜCEL

December, 2007
İZMİR

Ph.D. THESIS EXAMINATION RESULT FORM

We have read the thesis entitled "**MAGNETIC BEADS FOR CADMIUM REMOVAL FROM HUMAN PLASMA IN MAGNETICALLY STABILIZED FLUIZED BED (MSFB)**" completed by **NİLGÜN YÜCEL** under supervision of **Asst. Prof. Dr. M. Nalan TÜZMEN** and that in our opinion it is fully adequate, in scope and in quality, as a thesis for the degree of Doctor of Philosophy.

Asst. Prof. Dr. M. Nalan TÜZMEN
Supervisor

Prof. Dr. Adil DENİZLİ
Thesis Committee Member

Prof. Dr. Filiz KÜÇÜKSEZGİN
Thesis Committee Member

Examining Committee Member

Examining Committee Member

Approved by the
Graduate School of Natural and Applied Sciences

Prof.Dr. Cahit HELVACI
Director

ACKNOWLEDMENTS

I would like to thank my supervisor Asst. Prof. Dr. M. Nalan TÜZMEN, for her valuable advices and guidance.

I am also grateful to Prof. Dr. Adil DENİZLİ and his working team from Hacettepe University for his valuable supports and material auxiliary.

I am also thankful to Prof. Dr. Filiz Küçüksezgin and her coworkers to open your laboratory to me.

I must say a special thanks to my husband Tuna Yücel, who is a English teacher, for his excellent suggestions, which enabled met o correct a great many printing errors.

Finally, I would like to Express my appreciation to my family and my aunt Gülten Candan without their support and encouragement, this thesis would never have been completed certainly.

Nilgün YÜCEL

MAGNETIC BEADS FOR CADMIUM REMOVAL FROM HUMAN PLASMA IN MAGNETICALLY STABILIZED FLUIZED BED (MSFB)

ABSTRACT

The aim of this study is to prepare ion-imprinted magnetic beads which can be used for the selective removal of Cd^{2+} ions from Cd^{2+}-overdosed human plasma. N-methacryloyl-(L)-cysteinemethylester (MAC) was chosen as the complexing monomer. In the first step, Cd^{2+} was complexed with MAC and the Cd^{2+}-imprinted magnetic poly(HEMA-MAC) (mMIP) beads were produced by suspension polymerization in the presence of magnetite Fe_3O_4 nano-powder. After that, the template ions (i.e., Cd^{2+}) were removed from the polymer matrix using 0.1 M thiourea solution. The specific surface area of the mMIP beads was found to be 24.7 m^2/g with a size range of 63-140 μm in diameter and the swelling ratio was 70 %. The average Fe_3O_4 content of the resulting mMIP beads was 8.2 %. According to the elemental analysis results, the beads contained 41.8 μmol MAC/g polymer. The Cd^{2+} adsorption capacity decreased drastically from 48.8 μmol/g to 20.0 μmol/g with the increase of the flow rate from 0.50 ml/min to 3.0 ml/min. The maximum adsorption capacity was 48.8 μmol Cd^{2+}/g beads. Langmuir and Freundlich adsorption models were applied to describe the experimental isotherm and isotherm constants. Equilibrium data fitted very well to the Langmuir model in the entire concentration range (5-200 mg/L). The pseudo-first order and pseudo second order kinetic models were used to describe the kinetic data, and the rate constants were evaluated. The results showed that adsorption process of Cd^{2+} ions onto mMIP beads followed the pseudo second-order kinetic model. The relative selectivity coefficients of mMIP beads for Cd^{2+}/Pb^{2+} and Cd^{2+}/Zn^{2+} were 22.6 and 160.7 times greater than non-imprinted (mNIP) beads, respectively. The mMIP beads could be used many times without decreasing their adsorption capacities significantly.

Keywords: Affinity binding**,** Cadmium removal, Ion imprinting, Magnetic beads, Metal detoxification, Molecular recognition

MANYETİK OLARAK AKIŞKANLAŞTIRILMIŞ YATAK SİSTEMİNDE İNSAN PLAZMASINDAN KADMİYUM UZAKTIRILMASI İÇİN MANYETİK MİKROKÜRELER

ÖZ

Bu çalışmanın amacı; Cd^{2+}-aşırısı yüklenmiş insan plazmasından Cd^{2+} iyonlarının seçici olarak uzaklaştırılması için iyon-baskılanmış manyetik kürelerin hazırlanmasıdır. Metakriloamidosistein (MAC) kompleksleştirici monomer olarak kullanıldı. Bu amaçla çalışmanın ilk aşamasında, Cd^{2+}, MAC ile kompleksleştirildi ve Cd^{2+}-baskılanmış manyetik poli(HEMA-MAC) (mMIP) küreleri manyetik nano-tozu Fe_3O_4 varlığında süspansiyon polimerizasyonu ile üretildi. Daha sonra yapıdan kalıp (Cd^{2+}) 0,1 M tiyoüre çözeltisi kullanılarak uzaklaştırıldı. mMIP kürelerinin yüzey alanı 24,7 m^2/g, çapı 63-140 μm aralığında ve şişme oranları % 70 olarak belirlendi. Elde edilen mMIP kürelerinin Fe_3O_4 içeriği % 8,2 dir. Elementel analiz sonuçlarına göre, küreler 41,8 μmol MAC/g polimer içeriyorlardı. Kürelerin Cd^{2+} adsorpsiyon kapasitesi akış hızının 0,5 ml/dakika dan 3 ml/dakikaya artmasıyla 48,8 μmol den 20,0 μmol değerine keskin bir şekilde düşmüştür. Maksimum adsorpsiyon kapasitesi 48,8 μmol Cd^{2+}/g küredir. Langmiur ve Freundlich adsorpsiyon modelleri deneysel izoterm ve izoterm sabitlerini belirlemek için verilere uygulandı. Elde edilen sonuçların uygulanan konsantrasyon aralığında (5-200 mg/L) Langmuir modeli ile uygunluk gösterdiği belirlenmiştir. Yalancı 1. mertebe ve 2. mertebe kinetik modelleri kinetik verileri ve hız sabitlerini belirlemek için kullanıldı. Sonuçlar mMIP kürelerine Cd^{2+} iyonlarının adsorpsiyon prosesinin 2. mertebe kinetiğe uygunluk gösterdiğini belirlemiştir. Cd^{2+}/Pb^{2+} ve Cd^{2+}/Zn^{2+} nın mMIP kürelerine bağıl seçicilik sabitleri baskılanmamış (mNIP) kürelerinden sırasıyla 22,6 ve 160,7 kat daha fazlaydı. mMIP küreleri adsorpsiyon kapasiteleri önemli oranda düşmeksizin defalarca kullanılabilmektedir.

Anahtar Kelimeler: Afinite bağlanma, İyon baskılama, Kadmiyum uzaklaştırma, Manyetik küre, Metal Detoksifikasyonu, Moleküler tanıma

CONTENTS

Page

CHAPTER ONE

INTRODUCTION

1.1 Cadmium Physical and Chemical Properties

Cadmium (atomic number 48; relative atomic mass 112.40) is a metal that belongs, together with zinc and mercury, to group IIB in the Periodic Table. It is a relatively rare element and is not found in the pure state in nature. Cadmium is mainly associated with the sulfide ores of zinc, lead, and copper, although purification first took place in 1817 from zinc carbonate. Commercial production only became significant at the beginning of this century. Cadmium is often considered as a metal of the 20th century; indeed, over 65% of the cumulative world production has taken place in the last two decades (Wilson, 1988). Cadmium has a relatively high vapour pressure. Its vapour is oxidized rapidly in air to produce cadmium oxide. When reactive gases or vapour, such as carbon dioxide, water vapour, sulfur dioxide, sulfur trioxide or hydrogen chloride are present, cadmium vapour reacts to produce cadmium carbonate, hydroxide, sulfite, sulfate or chloride, respectively. These compounds may be formed in stacks and emitted to the environment. Some cadmium compounds, such as cadmium sulfide, carbonate, and oxide, are practically insoluble in water. There is, however, a lack of data on the solubility of these compounds in biological fluids, e.g., in the gastrointestinal tract and lung. These water-insoluble compounds can be changed to water-soluble salts in nature under the influence of oxygen and acids; cadmium sulfate, nitrate, and halides are water-soluble. Most of the cadmium found in mammals, birds, and fish is probably bound to protein molecules.

The speciation of cadmium in soil, plants, animal tissues, and foodstuffs may be of importance for the evaluation of the health hazards associated with areas of cadmium contamination or high cadmium intake. Very few data on the occurrence and speciation of cadmium compounds in nature are available. Cadmium is commonly regarded as a pollutant of worldwide concern. The metal has been reviewed by the International Register of Potentially Toxic Chemicals of the United

Nations Environment Programme. As a result, it has been included on the list of chemical substances and processes considered to be potentially dangerous at the global level.

1.1.1 Uses

Cadmium has a limited number of applications but within this range the metal is used in a large variety of consumer and industrial materials. The principal applications of cadmium fall into five categories: protective plating on steel; stabilizers for poly-vinyl chloride (PVC); pigments in plastics and glasses; electrode material in nickel-cadmium batteries; and as a component of various alloys. Detailed consumption statistics are only available for a limited number of countries but from these it is apparent that the pattern of use can vary considerably from country to country (Wilson, 1988). Examination of the reported trends in cadmium consumption over the last 25 years reveals considerable changes in the relative importance of the major applications. The use of cadmium for electroplating represents the most striking decrease in 1960 this sector accounted for over half the cadmium consumed worldwide, but in 1985 its share was less than 25 % (Wilson, 1988). In contrast, the use of cadmium in batteries has shown considerable growth in recent years from only 8% of the total market in 1970 to 37 % by 1985. The use of cadmium in batteries is particularly important in Japan and represented over 75 % of the total consumption in l985 (Wilson, 1988). Of the remaining applications of cadmium, pigments and stabilizers are the most important, accounting for 22 % and 12 %, respectively, of the world total in 1985. The share of the market by cadmium pigments remained relatively stable between 1970 and l985 but the use of the metal in stabilizers during this period showed a considerable decline, largely as a result of economic factors. The use of cadmium as a constituent of alloys is relatively small and has also declined in importance in recent years, accounting for about 4% of total cadmium use in l985 (Wilson, 1988).

1.1.2 Sources of Cd^{2+}, Environmental Levels and Human Exposure

Cadmium is a relatively rare element and current analytical procedures indicate much lower concentrations of the metal in environmental media than did previous measurements. At present, it is not possible to determine whether human activities have caused a historic increase in cadmium levels in the polar ice caps. Cadmium is widely distributed in the earth's crust at an average concentration of about 0.1 mg/kg. However, higher levels may accumulate in sedimentary rocks, and marine phosphates often contain about 15 mg cadmium/kg. Weathering also results in the riverine transport of large quantities of cadmium to the world's oceans and this represents a major flux of the global cadmium cycle; an annual gross input of 15 000 tonnes has recently been estimated (Friberg et al., 1992). Volcanic activity is a major natural source of cadmium release to the atmosphere. Emissions of cadmium take place both during episodic eruptions and continuous low-level activity. Difficulties exist in quantifying the global flux from this source but an estimate of 100-500 tonnes (Nriagu, 1979) has been made. Deep sea volcanism is also a source of environmental cadmium release, but the role of this process in the global cadmium cycle remains to be quantified. Ice and snow deposits from the polar regions represent a unique historical record of pollutants in atmospheric precipitation. However, the problems of contamination are great and no reliable data are at present available from historic samples; this prevents an insight into temporal changes in the cycling of cadmium. Nevertheless, current ice samples have been analysed; those from the Arctic contain on average 5 pg/g, while corresponding values from the Antarctic (0.3 pg/g) are much lower (Wolff & Peel, 1985). Commercial cadmium production started at the beginning of this century. The pattern of cadmium consumption has changed in recent years with significant decreases in electroplating and increases in batteries and specialized electronic uses. Most of the major uses of cadmium employ cadmium in the form of compounds that are present at low concentration; these features constrain the recycling of cadmium (Friberg et al., 1992). Restrictions on certain uses of cadmium imposed by a few countries may have widespread impact on these applications. Cadmium is released to the air, land, and water by human activities. In general, the two major sources of contamination are the

production and consumption of cadmium and other non-ferrous metals and the disposal of wastes containing cadmium. Areas in the vicinity of non-ferrous mines and smelters often show pronounced cadmium contamination. Increases in soil cadmium content result in an increase in the uptake of cadmium by plants; the pathway of human exposure from agricultural crops is thus susceptible to increases in soil cadmium. The uptake by plants from soil is greater at low soil pH. Processes that acidify soil (e.g., acid rain) may therefore increase the average cadmium concentrations in foodstuffs (Friberg et al., 1992). The application of phosphate fertilizers and atmospheric deposition are significant sources of cadmium input to arable soils in some parts of the world; sewage sludge can also be an important source at the local level. These sources may, in the future, cause enhanced soil and hence crop cadmium levels, which in turn may lead to increases in dietary cadmium exposure. In certain areas, there is evidence of increasing cadmium content in food. Edible free-living food organisms such as shellfish, crustaceans, and fungi are natural accumulators of cadmium. There are increased levels of cadmium in the liver and kidney of horses and some feral terrestrial animals, as in the case of humans. Regular consumption of these items can result in increased exposure Certain marine vertebrates contain markedly elevated renal cadmium concentrations, which, although considered to be of natural origin, have been linked to signs of kidney damage in the organisms concerned (Friberg et al., 1992).

1.2 Environmental Transport, Distribution, and Transformation

1.2.1 Atmospheric Deposition

Cadmium is removed from the atmosphere by dry deposition and by precipitation. Total deposition rates have been measured at numerous localities worldwide and values have generally been found to increase in the order: background < rural < urban < industrial (Friberg et al., 1992).

1.2.2 Transport From Water to Soil

Rivers contaminated with cadmium can contaminate surrounding land, either through irrigation for agricultural purposes, by the dumping of dredged sediments, or through flooding (Forstner, 1980). For example, agricultural land adjacent to the Neckar River, Germany, received dredged sediments to improve the soil, a practice that produced soil cadmium concentrations in excess of 70 mg/kg (Forstner, 1980).

1.2.3 Uptake From Soil by Plants

It has been shown repeatedly that an increase in soil cadmium content results in an increased plant uptake of the metal. This has been demonstrated for soils with naturally elevated cadmium levels (Lund et al., 1981), those contaminated by non-ferrous metal mining, and those that have received cadmium via sewage sludge applications (Davis & Coker, 1980). It is this basic relationship that makes the soil-crop pathway of human exposure susceptible to increased levels of soil cadmium. Indeed, since the major sources of cadmium exposure for the general population are food and tobacco, it is important to assess those soil and plant factors that influence cadmium uptake by crop plants. The most important soil factors influencing plant cadmium accumulation are soil pH and cadmium concentration (Davis & Coker, 1980). Soil cadmium is distributed between a number of pools or fractions, of which only the cadmium in soil solution is thought to be directly available for uptake by plants. Soil pH is the principal factor governing the concentration of cadmium in the soil solution. Cadmium absorption to soil particles is greater in neutral or alkaline soils than in acidic ones and this leads to increased cadmium levels in the soil solution. As a consequence, plant uptake of cadmium decreases as soil pH increases. Other soil factors that influence the distribution of cadmium between the soil and soil solution include cation exchange capacity and the contents of the hydrous oxides of manganese and iron, organic matter, and calcium carbonate. Increases in these parameters result in decreased availability of cadmium to plants owing to a reduction of the level of cadmium in the soil solution.

Much attention has been paid to the plant availability of cadmium in agricultural soils to which sewage sludge has been applied. It has been observed that the repeated application of sludge to soils can alter the availability of cadmium, and although soil cadmium levels may increase, crop levels do not always reflect this increase (Page et al., 1981). The long-term availability of cadmium to plants is uncertain, availability having been reported to remain constant, decrease, or even increase with time. In another study there were no clear changes in the plant availability of cadmium over a period of five years after sewage sludge was applied to the soil (Carlton-Smith, l987).

Concern over the long-term implications of present-day cadmium inputs to European arable soils has led to modelling studies of the future cadmium exposure for the general population. It was estimated by Tjell et al. (1981) that cadmium inputs from phosphate fertilizers and atmospheric deposition will cause an annual increase of 0.6 % in Danish soil cadmium levels. The corresponding increases in crop cadmium concentrations would lead to a predicted 70 % increase in dietary cadmium intake 100 years hence (Friberg et al., 1992).

1.2.4 Transfer to Aquatic and Terrestrial Organisms

In general, cadmium concentrations in terrestrial and aquatic biota from uncontaminated localities are low, corresponding to the geochemical abundance of this metal. However, in certain situations, cadmium displays a propensity for marked bioaccumulation, a feature that has implications for human dietary exposure and may be of toxicological significance for the organisms concerned. It appears that cadmium shows greatest mobility in certain marine ecosystems. Phytoplankton in areas of oceanic upwelling contain raised cadmium levels (Martin & Broenkow, 1975), and filter-feeding molluscs can accumulate significant concentrations of cadmium even in coastal localities that are only moderately contaminated. Oysters, in particular, are well-known cadmium accumulators, levels of up to 8 mg/kg wet weight having been recorded in New Zealand (Nielsen, 1975). Certain edible

crustaceans such as crab and lobster also contain relatively high cadmium concentrations, the metal being localized in the hepatopancreas or "brown meat" (Buchet et al., l983). Terrestrial mosses and lichens display a high capacity for retention of metals deposited from the atmosphere and these plants have been used to map both local contamination from point sources and regional patterns of cadmium deposition. The fruiting bodies of some macrofungi contain remarkably high cadmium concentrations even in areas uncontaminated with cadmium. This phenomenon has implications for human dietary exposure as some accumulator species are edible. In addition to humans, certain long-lived terrestrial mammals such as the horse and moose may possess considerable cadmium burdens in the kidney and liver (Elinder & Piscator, 1978; Frank et al., 1981; Jeffery et al., 1989). It has been shown that cadmium accumulates with age in horse kidney. High inhalation exposure to cadmium oxide fume results in acute pneumonitis with pulmonary oedema, which may be lethal. High ingestion exposure of soluble cadmium salts causes acute gastroenteritis. Long-term occupational exposure to cadmium has caused severe chronic effects, predominantly in the lungs and kidneys (Friberg et al., 1992). Chronic renal effects have also been seen among the general population. Following high occupational exposure, lung changes are primarily characterized by chronic obstructive airway disease. Early minor changes in ventilatory function tests may progress, with continued cadmium exposure, to respiratory insufficiency. As has occurred in the past, an increased mortality rate from obstructive lung disease has been seen in workers with high exposure. The accumulation of cadmium in the renal cortex leads to renal tubular dysfunction with impaired reabsorption of, for instance, proteins, glucose, and amino acids. A characteristic sign of tubular dysfunction is an increased excretion of low molecular weight proteins in urine. In some cases, the glomerular filtration rate decreases. Increase in urine cadmium correlates with low molecular weight proteinuria and in the absence of acute exposure to cadmium may serve as an indicator of renal effect. In more severe cases there is a combination of tubular and glomerular effects, with an increase in blood creatinine in some cases. For most workers and people in the general environment, cadmium-induced proteinuria is irreversible.

Among other effects are disturbances in calcium metabolism, hypercalciuria, and formation of renal stones. High exposure to cadmium, most probably in combination with other factors such as nutritional deficiencies, may lead to the development of osteoporosis and/or osteomalacia. There is evidence that long-term occupational exposure to cadmium may contribute to the development of cancer of the lung but observations from exposed workers have been difficult to interpret because of confounding factors. For prostatic cancer, evidence to date is inconclusive but does not support the suggestion from earlier studies of a causal relationship. At present, there is no convincing evidence for cadmium being an etiological agent of essential hypertension. Most data speak against a blood pressure increase due to cadmium and there is no evidence of an increased mortality due to cardiovascular or cerebrovascular disease (Friberg et al., 1992).

1.3 Environmental Levels and Human Exposure

Human uptake of cadmium occurs via the inhalation of air and the ingestion of food and drinking-water. Accidental ingestion of cadmium through the contamination of foods in contact with cadmium-containing materials has occurred in the past. Accidental high-level inhalation exposure during welding operations and cadmium smelting is still a considerable hazard. Chronic exposure to cadmium via food or workplace air is the main concern in assessing the health risks of cadmium (Friberg et al., 1992).

1.3.1 Inhalation Route of Exposure

1.3.1.1 Ambient Air

Many countries carry out regular monitoring programmes for cadmium in the air. An assessment of the available data from various European countries showed that average values range from 1 to 5 ng/m^3 in rural areas, 5 to 15 ng/m^3 in urban areas, and 15 to 50 ng/m^3 in industrialized areas (Friberg et al., 1992). Examination of some individual national data (Table 1) suggests that urban values are likely to occupy the lower end of the range indicated above. Much higher air cadmium concentrations are found in areas close to major atmospheric sources of the metal. However, these values can fluctuate widely as a result of changing emission characteristics and weather conditions. Studies of the particle size distributions of cadmium in urban aerosols generally show that the metal is associated with particulate matter in the respirable range (Greenberg et al., 1978). The enrichment of cadmium on these smaller particles can be linked to the behaviour of the metal in thermal facilities that are sources of airborne cadmium. An air quality study revealed no differences between indoor and outdoor air cadmium levels when the dwellings of non-smokers were examined. However, significantly higher indoor air cadmium levels were observed in those houses where smoking took place.

Table 1.1 Typical levels of cadmium in ambient air

Type of area	Cadmium concentration range (ng/m^3)	Period[b]	Sampling Reference
Remote rural			
Pacific atoll	0.0025-0.0046	NR	Duce et al. (1983)
Europe	0.1-0.3	NR	Heindryckx et al. (1974)
Atlantic	3×10^{-6}-6.2×10^{-4}	NR	Duce et al. (1975)
Rural			
Belgium	1[a]	24 h	Janssens & Dams (1974)
Germany	0.1-1	< 24 h	Neeb & Wahdat (1974)
Japan	1-4	24 h	Japanese Environment Agency (1974)
Urban			
Belgium	50[a]	24 h	Janssens & Dams (1974)
Germany	10-150	< 24 h	Neeb & Wahdat (1974)
Japan	3-6.3	1 year	Japanese Environment Agency (1974)
Poland	2-51	1 year	Just & Kelus (1971)
USA (New York)	3-23	1 year	Kneip et al. (1970)

[a] Mean value [b] NR = not reported

1.3.1.2 Air in The Working Environment

Elevated air cadmium levels arise in the smelting of non-ferrous metals and in the production and processing of cadmium-containing articles. The thermal operations associated with these processes are mainly responsible for producing cadmium dusts and, if temperatures are sufficiently high cadmium fume. Airborne cadmium concentrations found in the occupational setting vary considerably according to the type of industry and the specific working conditions in each plant (Tarasenko & Vorobjeva, 1973). Occupational exposure to cadmium is mainly by inhalation but includes additional intakes through food and tobacco. The total cadmium level in air varies according to industrial hygiene practices and type of workplace. There is an exposure-response relationship between airborne cadmium levels and proteinuria. An increase in the prevalence of low molecular weight proteinuria may occur in workers after 10-20 years of exposure to cadmium levels of about 20-50 $\mu g/m^3$ (Friberg et al., 1992). *In vivo* measurement of cadmium in the liver and kidneys of people with different levels of cadmium exposure have shown that about 10% of workers with a kidney cortex level of 200 mg/kg and about 50 % of people with a kidney cortex level of 300 mg/kg would have renal tubular proteinuria (Kjellström et al., 1984).

In general, only total air cadmium concentrations are monitored in the working environment; factors influencing respiratory absorption, such as the speciation of cadmium and the size distribution of the collected particles, are not taken into account. Cadmium-containing dust particles that are too large to be delivered to the pulmonary region of the lung can enter the gastrointestinal tract by mucociliary transfer (Friberg et al., 1992).

1.3.1.3 The Smoking of Tobacco

The tobacco plant naturally accumulates relatively high cadmium concentrations in its leaves. As a result, this material represents an important source of exposure for smokers. It has been reported that one cigarette contains about 1-2 µg cadmium

and that about 10% of the cadmium content is inhaled when the cigarette is smoked (Elinder et al., 1983). One study has suggested that modifications in cigarette construction and the increasing popularity of filter cigarettes have reduced cadmium exposure from this source in recent years (Scherer & Barkemeyer, 1983). Regional differences exist in the cadmium concentration of cigarettes, and lower values (0.1-0.5 μg) have been found in samples from Argentina, India, and Zambia (Elinder et al., 1983). Biological monitoring surveys of the general population have shown that cigarette smoking can cause significant increases in the concentration of cadmium in the kidney. Occupationally exposed workers who smoke tobacco may be subject to higher exposure levels than their non-smoking colleagues. This may be because the original content of tobacco can be considerably increased when handled during work. In addition, the hand-to-mouth route of exposure may be more important in workers who are tobacco smokers (Friberg et al., 1992).

1.3.2 Ingestion Routes of Exposure

1.3.2.1 Levels in Food

Food-borne cadmium is the major source of exposure for most people. Average daily intakes from food in most areas not polluted with cadmium are between 10-40 μg. In polluted areas it has been found to be several hundred μg per day (Friberg et al., 1992). In non-polluted areas, uptake from heavy smoking may equal cadmium intake from food. Based on a biological model, an association between cadmium exposure and increased urinary excretion of low molecular weight proteins has been estimated to occur in humans with a life-long daily intake of about 140-260 μg cadmium, or a cumulative intake of about 2000 mg or more.

The cadmium content of agricultural crops varies according to species, variety cultivated and season. The results of an extensive nationwide survey of cadmium in different classes of raw agricultural crops from uncontaminated localities illustrate the range of values encountered within and between crop classes (Wolnik et al.,

1983). It is evident that cadmium is a normal constituent of most foodstuffs (Table 1.2).

Table 1.2 Cadmium concentrations in the major types of crop from various regions of the USA[a]

Cadmium concentration (mg/kg wet weight)

Crop	Median Cd^{2+} concentration	Minimum Cd^{2+} concentration	Maximum Cd^{2+} concentration
Rice	0.0045	< 0.001	0.23
Peanuts	0.060	0.010	0.59
Soybeans	0.041	0.002	1.11
Wheat	0.030	< 0.0017	0.207
Potatoes	0.028	0.002	0.18
Carrots	0.017	0.002	0.13
Onions	0.009	0.001	0.054
Lettuce	0.017	0.001	0.160
Spinach	0.061	0.012	0.20
Tomatoes	0.014	0.002	0.04

[a] From: Wolnik et al. (1983).

Meat, fish, and fruit generally contain similar cadmium levels and values of 5-10 µg/kg fresh weight are representative for these food classes. Most plant-based foodstuffs contain higher cadmium concentrations and a value of 25 µg/kg fresh weight is considered representative for the staple items, cereals and root vegetables. Offal from adult animals and certain shellfish contain even higher concentration values in excess of 50-100 µg/kg fresh weight are considered normal. Food preparation can result in cadmium losses from plant-based items. The milling of wheat grain results in a reduction of about 50% in the cadmium content of the white flour produced The washing, peeling, and cooking of vegetables can also lead to reductions in the concentrations of cadmium but, in general, these are relatively small. The use of glazed ceramic containers to store foodstuffs can lead to significant cadmium contamination, particularly in the case of foods that are acidic liquids (Friberg et al., 1992).

1.4 Kinetics and Metabolism in Laboratory Mammals and Humans

1.4.1 Uptake

1.4.1.1 Absorption of Cd^{2+}

The retained or accumulated dose at the local or systemic target site resulting from the deposited dose may eventually lead to biological effects. Length of exposure is of major importance for chronic effects, particularly lung cancer. Data on the respiratory absorption of cadmium in humans comes largely from comparisons of smokers and non-smokers. On the basis of data on organ burdens of cadmium and smoking history, Elinder et al. (1976) calculated that about 50 % of the cadmium inhaled via cigarette smoke could be absorbed. A study in which cadmium chloride was given in drinking-water to rats over a period of 12 months showed retention in the kidney and liver of less than 1 % of the total amount ingested (Decker et al., 1958).

1.4.2 Transport

Human data on the transport of cadmium from the site of absorption to the various organs are not available. Immediately after parenteral administration, most of the cadmium was present in the plasma. Plasma concentrations decrease rapidly during the first hours after injection, reaching a level that is less than 1 % of the initial value at 24 h, and this level then decreases much more slowly (Friberg et al., 1992). During the early, fast-elimination phase, cadmium in mouse plasma is mainly bound to plasma proteins with a molecular weight of 40 000 to 60 000 (probably albumin), whereas in the slower phase (more than 24 h after injection), it is partly bound to a low molecular weight (LMW) protein of the same size as metallothionein (Nordberg, 1978). After rats were repeatedly exposed by subcutaneous injection (up to 14 weeks), the cadmium in plasma was partly bound to proteins with a molecular weight of 40 000 to 60 000 and partly to a LMW protein with a molecular weight similar to that of metallothionein. The proportion of plasma cadmium bound to metallothionein and larger proteins, respectively, is considered to vary with the length and type of exposure. The concentration of cadmium in blood cells increases rapidly after a

single intravenous injection (1 mg/kg body weight) and, within a few hours, reaches a first peak concentration exceeding that of the plasma. Although the levels of cadmium per cell may be 10 times higher in leucocytes than in red cells, the total cadmium in the leucocyte portion of the blood is negligible compared to that in the red cells (Friberg et al., 1992). Cadmium in erythrocytes may partly be bound to haemoglobin. However, during the first hour after a single subcutaneous injection, a large proportion of the cadmium in erythrocytes is bound to proteins with a molecular weight larger than haemoglobin. Between 96 and 196 h after a single injection (1 mg/kg body weight), it has been shown in rats, that cadmium is also bound to a LMW protein (Nordberg, 1984). A part of the erythrocyte cadmium in rats was also found in erythrocyte ghosts (membranes). When mice were exposed by subcutaneous injection to cadmium chloride (0.25 mg/kg body weight) for periods of between 6 days and 5 months, most of the erythrocyte cadmium was bound to a LMW protein similar to metallothionein. Since metallothionein-bound cadmium is quickly cleared from the plasma by the kidneys this LMW fraction may be of great importance for the transport of cadmium from liver to kidney during long-term exposure. Hepatic metallothionein may be released into the blood in the same manner as hepatic enzymes and transported to the kidney and urine in some types of hepatic disorders (Tanaka, 1982).

1.4.3 Distribution

Cadmium is stored to the greatest extent in the liver and kidneys, the renal cortex showing the highest concentration in people who have not been exposed to excess cadmium. The lowest concentrations (wet weight) are found in the brain, bone, and fat (Friberg et al., 1974). Cadmium levels in the organs of second and third trimester fetuses and in newborn babies and young children are lower by three orders of magnitude than in adult females. The placenta contains somewhat higher concentrations than maternal blood, brain or fat. It has been calculated that about a third of the body burden in a non-smoking male from the USA is in the kidney and about a quarter in the liver and muscles. These are the tissues with the longest biological half-time of cadmium. In spite of the low cadmium concentration in the

muscles, the contribution to the total body burden is great due to the large weight of the muscles. Other tissues that contribute significantly to body burden are bone, skin, and fat. In cadmium workers and people in the general environment exposed to high levels of cadmium, the liver or kidneys show the highest concentration, depending on exposure time, exposure levels, and the level of renal function (Kjellström et al., 1979).

1.4.4 Body burden and kidney burden in humans

The newborn baby is practically free of cadmium and the concentrations of cadmium in the organs increase with age (Elinder et al., 1976). For example, the geometric mean concentration of cadmium in the renal cortex of 117 adults aged between 30 and 59 in Stockholm was 19 mg/kg (Elinder et al., 1976). The critical organ in long-term exposure to low concentrations of cadmium is the kidney. Initial cadmium-induced effects occur mainly in the proximal tubules, situated in the cortex of the kidney. Therefore, cadmium concentrations in the renal cortex and the distribution of cadmium within the kidney are of key importance. The weight of the renal cortex is about 2-3 times greater than the weight of the renal medulla, and early estimates of renal cortex cadmium concentrations were 1.5 times higher than the whole kidney concentrations (Friberg et al., 1992).

1.5 Biological Half-time and Metabolic Models

Experimental and epidemiological evidence indicates strongly that the biological half-time in the whole body is extremely long (many years). Experimental evidence from one study (Shaikh & Smith, 1980), in which one subject was given radioactive cadmium and examined periodically for the next 2 years, showed a biological half-time of 26 years. In three similar studies, in which a small number of subjects were followed up for a limited period (about 100 days), half-times of 93-202 days were reported (Rahola et al., 1972; Flanagan et al., 1978; McLellan et al., 1978). Only one of these studies (Rahola et al., 1972) gave confidence limits for the estimated biological half-time (130 days to infinity). Another approach to estimate the half-

time used involves comparing total daily excretion with total body burden, applying a one-compartment model to the body as a whole. A further approach analyses the accumulation in the kidney using a one-compartment model taking into consideration age-related variations in daily cadmium exposure and kidney weight. More recently, an elaborate model has been developed that includes separate compartments for, for instance, kidney, liver, and blood, and incorporates age-related variations in daily intake, tissue weights, and renal function. These models rely on many assumptions concerning the cadmium concentration in food, calorific intake, absorption rates, and other factors. Inevitably, the data produced by these models are only tentative, but they are important for future research (Friberg et al., 1992).

1.5.1 Urine

In the absence of episodes of high-level exposure to cadmium and provided that cadmium-binding sites in the organism are not saturated and cadmium-induced nephropathy has not yet occurred, the urine cadmium level increases in proportion to the amount of cadmium stored in the body (Friberg et al., 1992). In such situations, which prevail mainly in the general population and in workers moderately exposed to cadmium, there is significant correlation between urinary cadmium and cadmium in kidney. Episodes of high exposure to cadmium, however, may lead to a transient increased urinary excretion. If exposure to cadmium has been excessive, the cadmium-binding sites in the organism become progressively saturated and, despite continuous exposure, the cadmium concentration in the renal cortex tends to plateau. Once this point is reached, the cadmium that is still absorbed cannot be further retained in the kidney and is rapidly excreted in the urine. Under these conditions, urinary cadmium is also influenced by the recent intake. The relative influence of the body burden and the recent exposure on urinary cadmium depends on the exposure intensity. If exposure continues, a certain percentage of individuals may develop renal damage. This is associated with a progressive loss of cadmium accumulated in the kidney, which gives rise to a further increase in urinary cadmium. Eventually, the amount of cadmium that can be released from the kidney decreases progressively and the urinary cadmium concentration follows the same trend. The changes in the

urinary metallothionein level parallel those of cadmium. In summary, several factors (duration and intensity of exposure to cadmium, the presence of renal dysfunction and its duration) must be taken into consideration when interpreting urinary cadmium (and metallothionein) levels (Friberg et al., 1992).

1.5.2 Blood

Plasma cadmium levels are considered to be related to recent exposure but are often so low that they cannot be measured routinely (Friberg et al., 1992). Most of the cadmium in the blood is in the erythrocytes. Cadmium levels in whole blood mainly reflect the exposure during recent weeks or months. In cadmium workers, the level increases markedly within the first few months after occupational exposure starts. It is probable that a portion of the blood cadmium level reflects body burden rather than present exposure in view of the known transport of cadmium via blood from the liver to the kidneys and other tissues and the long-term half-time component demonstrated by Jarup et al. (1983). Workers with relatively long exposure durations but whose cadmium exposure has ceased have elevated blood cadmium levels for several years. Reports of blood cadmium levels in the general population have, in the past, often been unreliable, owing largely to the difficulties encountered in the analysis of blood cadmium (Lauwerys et al., 1975). However, improvements in analytical techniques have since been achieved through biological standards for blood and systematic quality assurance programmes (Vahter, 1982). Average blood cadmium values up to 10 μg/litre or more have been reported in the past, but the analytical procedures used mean that the accuracy of these data is in doubt (Vahter, 1982). It was found that even in the countries with the highest blood cadmium levels, the average was less than 4 μg/litre. Furthermore, smokers were found to have higher values than non-smokers, and non-smokers, in most countries, had mean levels below 1 μg/litre. Although only slightly above 1 μg/litre, the levels for non-smokers in Japan were about twice as high as the levels in the USA, which probably reflects the difference in average daily cadmium intake via food. Reported cadmium concentrations in the blood of exposed workers are generally between 5 and 50

μg/litre, but levels of between 100 and 300 μg/litre have resulted from extreme exposures (Friberg et al., 1992).

*1.5.3 Faec*es

Gastrointestinal absorption amounts to only a few percent of the cadmium ingested daily, and the quantity of cadmium excreted gastrointestinally is small compared to the unabsorbed portion of ingested cadmium. Thus, daily faecal cadmium can serve as a good indicator of the daily amount of cadmium ingested via food and water or cleared from the lungs after occupational exposure to large dust particles. Faecal cadmium correlates very closely with daily energy intake and average cadmium intake estimates for different countries agree well with reported average faecal cadmium amounts. A portion of the cadmium in human faeces is related to the body burden. In workers with high body burdens but low daily cadmium intakes via food, this portion might be greater than the unabsorbed part of ingested cadmium, because the faecal excretion is similar to the urinary excretion (Friberg et al., 1992).

1.6 The Role of Metallothionein in Transport, Metabolism, and Toxicity of Cadmium

Metallothionein is a metal-binding protein of low molecular weight, which has a key role in the metabolism of cadmium. It is rich in cysteine but contains no aromatic amino acids or histidine. This protein was identified for the first time by Margoshes & Vallee (1957) in horse kidney cortex. Its molecular weight is about 6600 (6000 for the apoprotein moiety, thionein), and it has a non-globular shape. On gel filtration, however, it moves like a spherical protein with a molecular weight of about 10 000. Piscator (1964) suggested that metallothionein played a role in cadmium transport and detoxication, and it has subsequently been identified in human kidney and liver as well as in those of various experimental animals. The structure and genetic expression of mouse and human metallothionein have now been identified. Two

major forms of metallothionein are present in most mammalian tissues, particularly liver and kidney, i.e. metallothionein I (Mt-I) and metallothionein II (Mt-II). Induction of synthesis is under the control of a large group of genes and is stimulated by glucocorticoids and the essential metals zinc and copper, as well as by the toxic metals cadmium and mercury. *In vitro* binding affinities have been demonstrated for a number of other toxic metals, including bismuth, cobalt, silver, and gold. Metallothionein binds seven metal ions per molecule between two separate metal-cysteine clusters, and a single molecule may contain more than one metal, e.g., cadmium and zinc, mercury and copper (Friberg et al., 1992). Piscator (1964) suggested that some of the cadmium-binding metallothionein in the liver may migrate into the blood stream. Plasma cadmium in animals exposed for a long time to cadmium is bound to a protein with the same molecular weight as metallothionein. When metallothionein-bound cadmium is present in the plasma, it is quickly cleared by glomerular filtration and reabsorbed in the renal tubules or excreted in the urine (Nordberg et al., 1975). At low levels of cadmium-metallothionein in the plasma, tubular reabsorption is almost complete, whereas the uptake in the tubular cells from the tubular fluid is saturated in the presence of high concentrations. Thus, high urinary excretion of cadmium-metallothionein occurs shortly after the administration of larger doses, i.e. doses exceeding about 0.1 mg cadmium/kg body weight. It has been demonstrated in animal and *in vitro* tissue studies that metallothionein provides a protective role for cadmium toxicity. Mice pretreated with cadmium have increased tolerance to subsequent cadmium exposure and exposure to cadmium may protect from subsequent mercury toxicity. In addition, the inhibition of certain mixed-function oxidases by cadmium is reduced by prior induction of metallothionein by cadmium in immature mice (Asokan et al., 1981). The renal tubular cell toxicity produced by metallothionein with different ratios of cadmium and zinc is proportional to the cadmium content of the metallothionein. Zinc-thionein does not have a similar effect. The prevalence of nephrotoxicity rather than hepatotoxicity in chronic cadmium exposure may be due to several factors. Firstly, the release of hepatic cadmium-metallothionein or its presence in the blood can result in preferential accumulation of cadmium in the kidneys. Secondly, it has been shown in experimental animals that the kidney can accumulate metallothionein mRNA in

response to cadmium exposure to only about half the level of the liver. Thus, the kidney may not be able to synthesize metallothionein as efficiently as the liver in response to cadmium exposure, resulting in an accumulation of non-metallothionein cadmium in the kidney but not in the liver. Most cadmium in human urine is bound to metallothionein (Tohyama et al., 1981), and good correlation has been found between the urinary cadmium and metallothionein concentrations both in elderly women exposed in the general environment (Tohyama et al., 1981) and in male cadmium workers. Measurement of urinary metallothionein thus provides a good indication of the urinary cadmium level and offers the advantage over cadmium analysis of avoiding the possibility of external contamination. Women were found to have much higher urinary metallothionein concentrations than men, even at similar cadmium levels (Friberg et al., 1992).

1.7 Effects on Humans

Exposure to cadmium produces a wide variety of effects involving many organs and systems. From the point of view of preventive medicine, the detection of early effects on the kidneys is of particular importance in order to prevent more serious renal effects and those on the lungs or bones. Recent studies have been indicated that chronic exposure to cadmium may give rise to cancer (Friberg et al., 1992).

1.7.1 Acute Effects

1.7.1.1 Inhalation

Acute cadmium poisoning and, in some cases, death have been reported among workers shortly after exposure to fumes when cadmium metal or cadmium-containing materials have been heated to high temperatures. The principal symptom in acute cases, both fatal and non-fatal, is respiratory distress due to chemical pneumonitis and oedema (Lucas et al., 1980). At an early stage, the symptoms may be confused with those of "metal fume fever". In working environments where cases of acute poisoning occurred, cadmium concentrations were usually very high (Friberg et al., 1992).

1.7.1.2 Ingestion

Food contamination arose when acid foods and drinks were prepared and stored in contact with cadmium-plated surfaces. Rapid onset with severe nausea, vomiting, and abdominal pain were characteristic symptoms. Effects also occurred following the consumption of drinks with a cadmium concentration of approximately 16 mg/litre from an automatic vending machine in which drinking-water was cooled in a tank constructed with cadmium-containing solder (Nordberg et al., 1973). Recovery from acute poisoning appears to be rapid and complete. The amount of cadmium absorbed is probably very limited due to vomiting and the consequential short presence of cadmium in the gastrointestinal tract (Friberg et al., 1992).

1.7.2 Chronic Effects

Lower cadmium concentrations with longer periods of exposure than those described above will cause chronic cadmium poisoning. Fully developed poisoning among industrial workers shows two main effects: renal dysfunction and emphysema. The kidney is most frequently the critical organ, but under certain conditions (short-term peak exposures) it may be the lung. For people in the general environment, exposure is usually by the oral route and the kidney is the critical organ (Friberg et al., 1992).

Renal dysfunction is one of the characteristic signs of cadmium poisoning, and many cadmium workers have developed proteinuria, renal glucosuria, and aminoaciduria. In working environments with high cadmium exposure levels, workers have also developed hypercalciuria, phosphaturia, and polyuria and some have suffered from renal colic due to recurrent stone formation (Lauwerys et al., 1979). The polyuria is due to loss of urinary concentrating ağabeylity. In most of the early cases, only proteinuria, mild in comparison with the proteinuria in many other renal disorders, has been reported as a sign of renal dysfunction, and other signs of kidney dysfunction were not evident. Proteinuria is known to be an early sign of

cadmium poisoning, but the degree of proteinuria varies with time. According to recent observations using quantitative proteinuria methods, total proteinuria in 19 workers had not changed 4 years after exposure ceased (Friberg et al., 1992). In those 11 workers for whom urinary $ß_2$-microglobulin was measured before and after cessation of exposure, an increase was invariably seen. Eight of the workers had abnormal $ß_2$-microglobulin levels before exposure ceased, whereas three had normal levels before and developed abnormal levels after cessation. It can be concluded that cadmium-induced tubular proteinuria is irreversible in most workers, at least for several years. A marked increase in urine cadmium level may reflect cadmium-induced nephropathy if exposure has been chronic and correlates with low molecular weight proteinuria (Lauwerys et el., 1979). Existing studies of mortality from nephritis/nephrosis have been based upon epidemiological studies of renal failure given as the underlying cause of death on death certificates (Friberg et al., 1992). With the advent of kidney dialysis and transplantation, patients with kidney failure frequently survive and die of other causes. If kidney failure is indicated at all on their death certificates, it is frequently given as a contributing rather than underlying cause of death (Friberg et al., 1992). Renal tubular brush border enzymes may also be excreted in chronic cadmium poisoning. In patients with Itai-itai disease, urinary trehalase activity correlates inversely with tubular resorption of phosphorus and there is a statistical correlation between urinary trehalase and other urinary indicators of renal tubular dysfunction, such as glucose, $ß_2$-microglobulin, cadmium, and alpha-amino nitrogen, in inhabitants of chronic cadmium-polluted areas in Japan. Other renal effects in cadmium workers include glucosuria, aminoaciduria, impaired concentrating abilities, and hypercalciuria, which may cause disturbances in bone and calcium metabolism. The hypercalciuria leads to renal stone formation in some workers. An increased excretion of amino acids, particularly of serine and threonine, has been shown in industrial workers, but the amino acid excretion pattern was not consistent. In a cadmium worker with osteomalacia, there was an increase excretion of hydroxyproline, which could be an effect of changes in collagen metabolism related to the bone disorder (Friberg et al., 1992).

1.7.2.1 Disorders of Cadmium Metabolism and Bone Effects

Bone disease and abnormalities of calcium metabolism from exposure to cadmium in the general environment have only been noted in people in Japan with the clinical syndrome referred to as Itai-itai disease. The main characteristics of the disease are osteomalacia and osteoporosis with a tendency to fractures accompanied by severe pain and renal tubular dysfunction. Osteomalacia is characterized by inadequate mineralization of bonematrix, resulting in an increase in the relative amount of osteoid tissue. It represents the adult counterpart of childhoodrickets (Robbins et al. 1984). Osteoporosis is defined as an excessive but proportional reduction in the amounts of both the mineral and matrix phases of bone unaccompanied by any abnormality in structure of the residual bone.

Itai-itai disease is an endemic bone disease prevalent in the basin of the Jinzu river, which runs through the central part of Toyama Prefecture in West-Central Japan. It is characterized by osteomalacia in combination with renal tubular dysfunction in most cases. Patients also have osteoporosis and one of the most characteristic symptoms is severe bone pain. Hagino & Yoshioka (1961) reported that high concentrations of cadmium, lead, and zinc were present in autopsy tissues from people with Itai-itai disease and in the everyday foods of the endemic area.

1.7.2.2. Mechanism of Cadmium-induced Bone Effects

The available data show that cadmium can affect calcium, phosphorous, and bone metabolism in both industrial workers and people exposed in the general environment. These effects may be secondary to the cadmium effects on the kidneys but there have been few studies of calcium metabolism in people with excess exposure to cadmium. The increased prevalence of renal stones reported from certain industries is probably one manifestation of the cadmium-induced kidney effects. It is not known if factors other than cadmium play a role. Nogawa et al. (1987) reported that serum 1,25-dihydroxy- vitamin D levels were lower in Itai-itai disease patients

and cadmium-exposed subjects with renal damage than in non-exposed subjects. It is known that normal calcium absorption in the intestines and normal bone mineralization is dependent upon 1,25-dihydroxycholecalciferol. Vitamin D_3 taken into the body is converted to 25-hydroxy-vitamin D_3 in the liver, and then to 1,25-dihydroxy-vitamin D_3 in the mitochondria of renal proximal tubular cells, this being the biologically active species. Cadmium accumulates in the proximal tubular cells, depressing cellular functions, and this may result in reduced conversion of 25-hydroxy-to 1,25-dihydroxy-vitamin D_3. This is likely to lead to decreased calcium absorption and decreased mineralization of bone, which in turn may result in osteomalacia (Friberg et al., 1992).

1.7.2.3 Respiratory System Effects

Cadmium workers may develop chronic injury to the respiratory system, depending on the level and nature of exposure. The development of such effects is often quite slow, so that they are apparent only after several years of exposure. The rate of development and severity appear to be roughly proportional to the time and level of exposure. The effects on the lung increases the mortality of cadmium workers with high exposures. In the latter study, the mortality for bronchitis as related to the intensity of exposure, the group with the highest exposure having a highly significant (almost 4-fold) excess risk (observed 13) (Friberg et al., 1992).

1.7.2.4 Cancer

The International Agency for Research on Cancer and the US National Toxicology Program have both concluded that there is adequate evidence that cadmium is a human carcinogen. This designation as a human carcinogen was prompted primarily by repeated findings of an association between occupational cadmium exposure and lung cancer, as well as very strong rodent data, which included the pulmonary system as a target site. Thus, the lung is the most definitively established site of human carcinogenesis from cadmium exposure. In some studies, occupational or environmental cadmium exposure has also been associated with

development of cancers of the prostate, kidney, liver, hematopoietic system and stomach. Clearly, further epidemiological and experimental work is necessary to determine the target sites and nature of the carcinogenic risk from cadmium exposure to humans.

1.8 Molecular Imprinting

Molecular imprinting, first reported by Wulff and Sarhan (1972), is regarded as one of the most facile methods to introduce molecular recognition sites into polymeric membranes (Wulff, 1995; Mosbach & Ramström, 1996; Sellergren, 1997; Piletsky et al., 1999). In other words, the molecular memory, which is both the shape of the target molecule and alignment of the functional moieties to interact with those in the target molecule, are memorized in the polymeric materials for the recognition or separation of target molecule during formation of the polymeric materials themselves. The scheme for the former molecular imprinting has been given in Figure 1.1. (Yoshikawa et al.,1994)

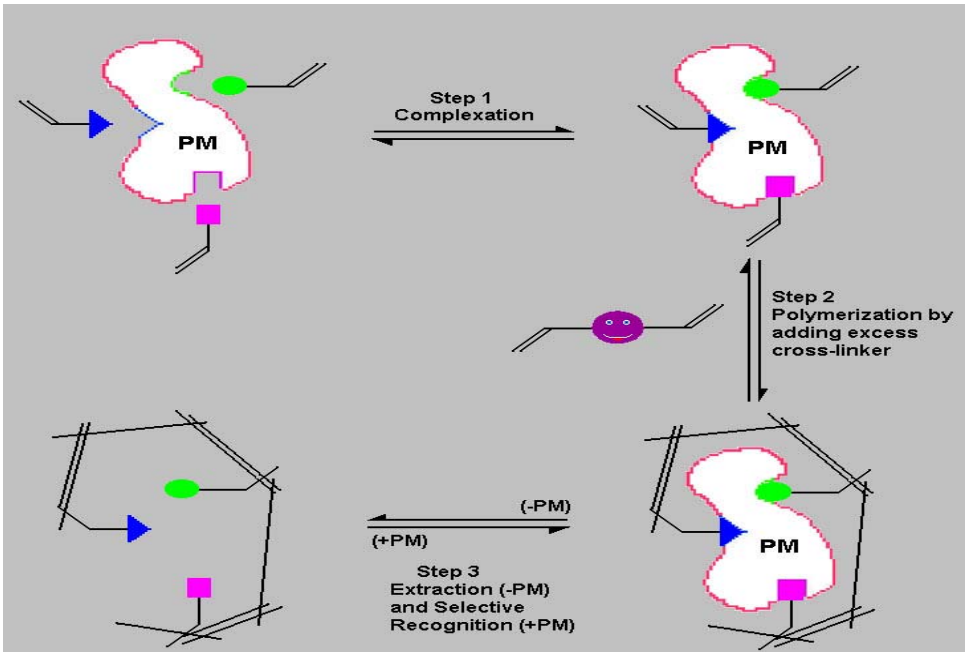

Figure 1.1 Schematic representation of the imprinting of specific cavities in a crosslinked polymer by a print molecule (PM) with three different functional groups.

In order to introduce molecular recognition sites into polymeric materials, the first step (Step 1) involves the complexation of a target molecule (a print molecule or a template) with polymerizable monomers having functional moieties, which form covalent or non-covalent bonds with the print molecule in solution. During this step, functional monomers are assembled around the print molecule and, as a result, predetermined orientation of the functional moieties is achieved. In the following step (Step 2), cross-linkers are added to the complex solution with the mixture being polymerized to form highly cross-linked polymers such that the molecular shape of the print molecule and alignment of the functional moieties may be retained in the molecularly imprinted polymeric materials thus prepared. Removal of the print molecule from the imprinted polymers leads to completion of the complementary molecular recognition sites. In other words, the print molecule fits into pockets in which the shape of the target molecule and alignment of the functional moieties are optimally set for recognition, i.e., 'tailor-made' binding sites. Single or multiple interactions of functional groups of both compounds can describe the interaction between analytes and/or template molecules and the monomers. The types of interaction can be hydrogen bonds, ion pairing, interaction or driven by the hydrophobic effect. The selection of the monomer(s) is based on the generation of these particular interactions. This implies that polymers generated from these monomers will always interact with the analyte or template molecule as well as with compounds that contain functional groups similar to those of the template.

The affinity increases with the number of interacting groups, however, each individual interaction can be strongly dependent on the properties of the solvent, *e.g.* protic or aprotic, polarity, dielectric constants, presence of complex forming agents, etc. These effects can occur through interaction with the polymer, the analyte or both. This implies that affinities can vary from zero to nanomolar equilibrium dissociation constants. Therefore, application of molecular imprints appears to have potential for a range of analytical applications. Nowadays, molecular imprinting may be classified into two categories 'pioneering molecular imprinting' and 'alternative molecular imprinting', which are used to tell apart pioneering molecular imprinting

from the latter case. The former is further divided into two categories, namely ‘covalent molecular imprinting’ and ‘non-covalent molecular imprinting’.

1.8.1 Covalent Molecular Imprinting

As for covalent molecular imprinting, covalent interactions, e.g., through formation reactions of boronic esters (Wulff & Sarhan 1972; Wulff et al.,1986), Schiff base formation (Wulff, 1982), ketal formation (Shea and Dougherty, 1986), esters (Sellergren & Andersson, 1990), and amides (Wulff et al., 1973) has been adopted. It is easy to obtain imprinted polymers with high specificity, due to stable complexes (covalent binding moieties) between the print molecule and target molecule being retained during polymerization. The covalent bond adopted for molecular imprinting should be reversible. Furthermore, formation and cleavage of the covalent bond should be fast for applications requiring membrane separation. This is, of course, also required in other applications.

1.8.2 Non-covalent Molecular Imprinting

Non-covalent molecular imprinting was proposed by Mosbach (1998; Arshady & Mosbach, 1981). The following interactions are enumerated as typical non-covalent interactions: hydrogen bonds, electrostatic interactions, hydrophobic interactions, metal coordinations, charge transfers, etc. Those non-covalent interactions should be, as a matter of course, reversible. Given the fact that non-covalent molecular interactions are prevalent in the biological world, exploitation of these binding forces, as it has turned out, has proven to be the most efficient and preferred method for generating robust, biomimetic binding materials (Mosbach et al., 2001). It is assumed that a change in selectivity of molecular imprinted polymers in comparison to non-imprinted polymers can only occur when the analyte and/or the matrix components of the sample will have an increased number of interaction points. So, single and part of the dual point interactions that take place between the analyte and the polymer will affect the selectivity. Note that non-imprinted polymers are successfully used for analytical applications. In other cases, the interaction of analytes and matrix components with non-imprinted parts of a polymer may

overshadow the interactions of the analyte with the true imprint so that the selectivity is not as good as required for the application, irrespective of the imprinting efficacy. The number of binding sites present in the polymer that play a role in the selective interaction of the analyte with the imprint (cavity) is typically less than 1% but can mount to 35% of the theoretical maximum amount of binding sites. For that reason the impact of both the selective (imprinted part of polymer) and the non-selective (non-imprinted part of the polymer) interactions on the applicability of imprinted polymers in different analytical techniques is discussed here. A schematic representation of the selective and the non-selective interactions is given in Figure. 1.2.

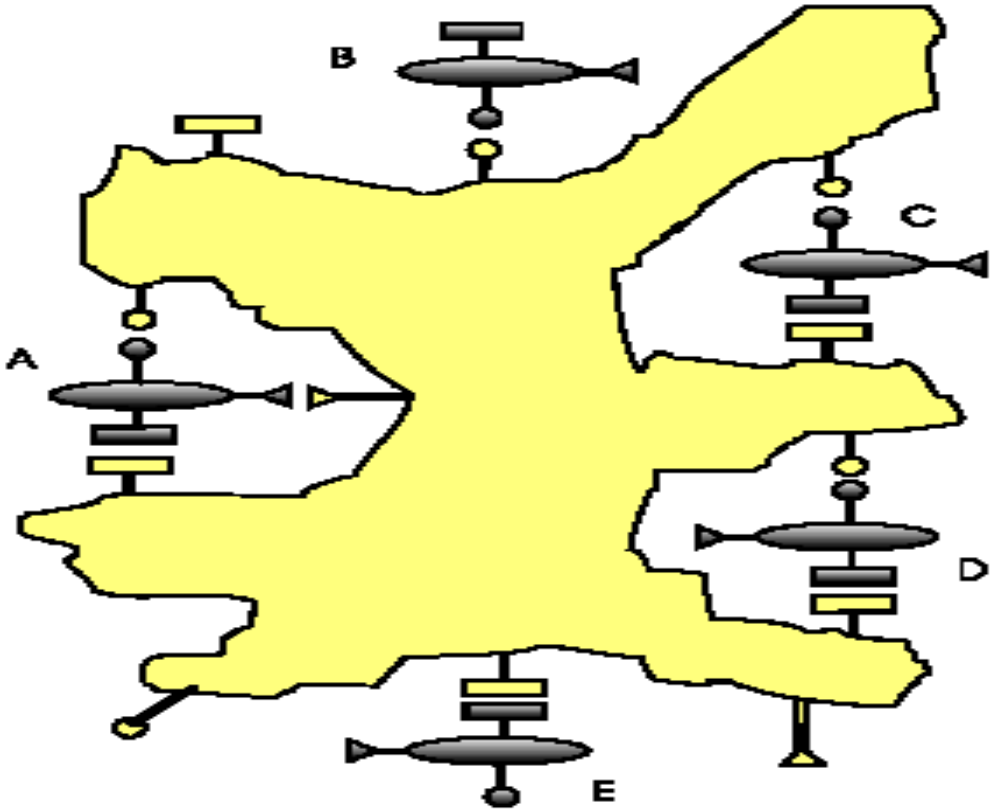

Figure 1.2 Schematic representation of the interaction of the analyte and the synthesized polymer. The polymer contains several binding sites. The most favorable energetic interaction is shown at location A, where three binding sites result in the most selective (specific) interaction of the analyte with the polymer. Two-point interactions, which are energetically less favorable, are depicted at locations C and D, where the analyte is still allowed to approach the binding sites at more than one way, and thereforeis less selective in its interaction with the polymer. Locations B and E show the least selective interaction possible and are therefore the least favorable. (Ensing, 1999)

1.8.3 Alternative Molecular Imprinting

As can be seen, molecular imprinting as described above is regarded to be one of the most facile methods to introduce molecular recognition sites into polymeric materials, but it has a number of points, which can be improved. The polymeric materials prepared by the molecular imprinting technique mentioned above are highly cross-linked polymers and thus would not be dissolved in any solvent. This means that the molecularly imprinted materials are not regenerable. In other words, once the molecularly imprinted materials, of which recognition sites are prepared for the recognition of a given target molecule, fall into disuse, such materials cannot be applied to the recognition of other molecules, and will thus have to be discarded. In addition to this, diversity of molecularly imprinted materials is not expected. Furthermore, in the author's personal opinion, cross-linking is not always necessary in order to fix the molecular motion of the imprinted polymers so as to retain the formed molecular recognition sites through using the knowledge of polymer physics. Based on this, another molecular imprinting method, which is called alternative molecular imprinting, was proposed in 1994 (Yoshikawa et al., 1994).

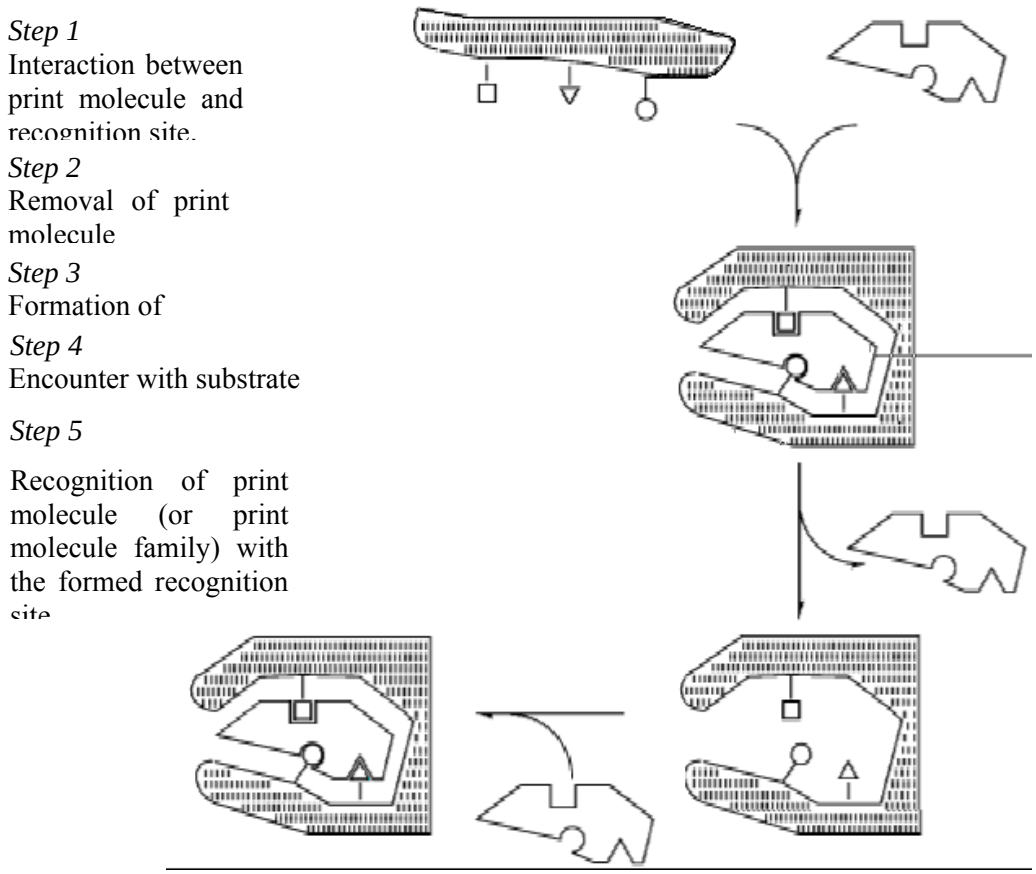

Figure 1.3 Shematic representation of alternative molecular imprinting.

Alternative molecular imprinting may be taken to be an extension of a bio-imprinting. In the bio-imprinting technique, existing recognition sites in an enzyme might be modified through the presence of a print molecule, while alternative molecular imprinting converts candidate materials with no molecular recognition sites into recognition materials. The concept of alternative molecular imprinting is shown in Figure 1.3.

Step 1 shows the specific interaction of the print molecule with the polymeric material, which is a candidate material to form molecular recognition sites, before and during the preparation process of molecular recognition materials in order to incorporate molecular memory into the polymeric materials. In Step 2, the print molecule is extracted from the molecularly imprinted material to complete preparation of the molecularly imprinted polymeric material (Step 3). When the print

molecule or print molecule analogue is in contact with the imprinted materials (Step 4), the recognition site preferentially interacts with them or incorporates them into the molecular recognition site (Step 5). Contrary to the pioneering molecular imprinting method, molecular recognition sites are formed at the same time as the molecular imprinting materials are prepared from the polymer solution. In other words, any polymer can be directly converted into a molecular recognition material by applying the alternative molecular imprinting without any requirement of delicate laboratory work. However, candidate polymeric materials should have the following properties: they are soluble in the imprinting solvent, while they should show solvent resistance toward solvent or solutions in which the application is taken place. Otherwise, swelling of the material leads to structural deformation of the recognition site, which is prepared by the presence of a print molecule. In order to prevent structural deformation of the formed recognition sites and to retain the 'molecular memory' in the molecularly imprinted material, candidate polymeric materials show a glassy state or possess high crystallinity, which play an important role in physical crosslinking under experimental conditions. Molecular recognition sites can be introduced into various polymeric materials, such as oligopeptide derivatives, derivatives of natural polymer, and synthetic polymers. In addition to this, as expected from the formation mechanism of imprinted materials, once the molecularly imprinted polymer, which is prepared for the recognition of a given target molecule, falls in disuse, the imprinted material can be dissolved and converted into another molecular recognition material by adopting a different target molecule as a print molecule. In other words, molecularly imprinted materials prepared using the alternative molecular imprinting methods are regenerable. Because MIPs have outstanding advantages such as predetermined selectivity, simple and convenient preparation, robustness in organic solvents and acidic or basic reagents, and durability to high temperature, molecular imprinting has drawn extensive attention in recent years. MIPs have been applied as affinity chromatographic stationary phases, artificial antibodies, synthesis mediators, sensor components and adsorbents for solid phase extraction. In principle, every compound could be made a corresponding MIP. However, up to now, only a limited number of compounds have been used for molecular imprinting. For the time being, MIPs are largely prepared on the basis of

trial and error. In order to obtain a MIP having high selectivity, which kind of structure a template should have, is one of the hot topics (Zhang et al, 2001).

1.9 Applications for Molecular Imprinted Polymers

In recent times, four main areas of application application for molecularly imprinted polymers have been pursued: (1) Affinity Separation, (2) Antibody Binding Mimics, (3) Enzyme Mimics and (4) Bio-Mimetic Sensors. These four areas continue to be the focus of most research efforts.

1.9.1 Affinity Separation

Affinity separation is the single biggest application for imprinted polymers at present (Mosbach et al., 1998). In this context, their use as stationary phases in high performance liquid chromatography (HPLC) continues to be an important research avenue, in spite of its well-documented (current) limitations: low capacity and heterogeneous binding sites. In the research laboratory, HPLC using an imprinted stationary phase remains one of the most convenient methods for assessing the efficiency of a new imprinting protocol. Besides liquid chromatography, it is very noticeable that imprinted polymers as selective solid-phase extraction (SPE) media are very much in vogue. It may well be that this is the area in which we will see the first commercial application of these materials. Other key lines of research in the affinity separation area include membranes and capillary electrophoresis (CE).

1.9.2 Antibody Binding Mimics

The demonstration that the strength and the selectivity of binding between an imprinted polymer and an analyte could be comparable, and in some cases even better than that between an antibody and an antigen generated enormous interest (Vlatakis et al, 1993). In an application sense, these antibody binding mimics (‘plastic antibodies’) offer a rapid and inexpensive route into stable and robust molecular recognition matrices (Haupt & Mosbach, 1998). They promise a real (non-immunogenic) alternative in applications that use antibodies in their insoluble form,

e.g. immunoaffinity chromatography (c.f. affinity separation above), immunosensors (cf. Bio-mimetic sensors below) and immunoassays. Some recent immunoassay-related studies have focussed on developing new assay formats that do not rely upon radioligands, e.g. fluorescence and electro chemical assays.

1.9.3 Enzyme Mimics

A dream for many working in the area of molecular imprinting has been to develop catalytically active imprinted polymers ('plastic enzymes') that are capable of mimicking Nature's enzymes. This task is, of course, an enormous undertaking, and the results reported to date tend to reflect this fact. Several different organic reactions have been successfully catalysed with molecularly imprinted polymers, including aldol condensations, ester hydrolyses, Diels–Alder reactions and β-eliminations. While molecularly imprinted polymers may not yet be able to compete with enzymes in terms of catalytic rate enhancements, they offer properties that are quite distinct from those of enzymes, e.g. their ready compatibility with organic solvents and their high temperature stability. Thus they are more useful as a complement to enzymes rather than as a replacement, at least for now.

1.9.4 Bio-mimetic Sensors

For some time now, there have been several concerted attempts to make in-roads into the biosensor market with imprinted polymers. The idea is, of course, to replace 'delicate' molecular recognition entities based on biomolecules with imprinted polymers (Kriz, 1997). Although the biosensor field is a very competitive area, one would expect molecularly imprinted polymers to challenge very strongly in this area given their many and varied attractive properties. Several potential applications have been demonstrated on a laboratory scale, but nothing, as yet, has found its way into the marketplace. Perhaps this is not so surprising bearing in mind the relatively tender age of this approach (Mosbach & Cormack, 1999).

1.10 Preparation Methods of Molecularly Imprinting Polymers

Imprinted polymers are usually prepared by bulk polymerization methods which produce a solid macroporous block which then must be crushed, ground and sieved to obtain a desired particle size. This is a tedious time consuming process. Furthermore, the properties of the resulting irregular particles may not be ideal with regard to flow, reproducibility, and scale-up procedures, whereas suspension polymerisation methods result in more suitable products. The particles should be spherical and uniform in size to minimize mass transfer limitations. Since the column separation efficiency increases with decreasing particle size, the size should be as small as possible. The pressure loss is minimal in columns packed by particles with spherical shape. Different groups have therefore tried suspension polymerisation methods. The main problem is the necessity to evaluate the compatibility of the conditions used for polymerisation with those required for complex formation between functional monomers and templates. Usual non-covalent interactions like hydrogen bonding or electrostatic interactions are not stable in aqueous suspension in which usually suspension polymerisation is carried out. Only with stable bonding like covalent interaction this has been applied. Water can be avoided by using a type of inverse suspension polymerisation in a very non-polar solvent like fluoro carbons. The disadvantage of this method is the high price of these solvents.

Table 1.3. lists the different imprinting methods that lead to polymer beads with various size ranges (Mosbach et al., 2001).

Method	Description	Advantage	Disadvantage
Normal Suspension Polymerisation	Suspension polymerisation in aqueous continuous phase.	Normal surfactants may satisfy formation of polymer beads that can be used for column chromatography.	the necessity to evaluate the compatibility of the conditions.
Suspension Polymerisation in perfluorocarbon	Suspension polymerisation in perfluorocarbon continuous phase.	Applicable to most imprinting systems, particle size adjustable.	Specialised surfactant needed.
Seed polymerisation	Polymerisation following multi-step swelling of seed particles.	Uniform polymer beads can be obtained for column chromatography.	Complicated multi-step swelling steps; not generally compatible to non-covalent imprinting systems.
Graft Polymerisation	Grafted imprinted polymer layer on supporting beads.	General compatibility with imprinting, uniform beads can be obtained for column chromatography.	Low loading capacity and grafting yield.
Precipitation Polymerisation	Cross-linking polymerisation starting from a dilute monomer solution.	Clean, uniform microspheres are generally obtained in good yield, the microspheres are easy to handle in drug assays.	Solvent condition need to be adjusted to minimise consumption of the print molecule.

Another possibility is the precipitation polymerisation, e.g., in acetonitrile with a colloidal stabilizer, like per-fluorinated polymeric surfactant. Thus rather small particles can be obtained. With special solvents like cyclopentanone or DMSO even soluble crosslinked beads containing molecular imprints having a similar diameter, as enzymes (5–10 nm) can be prepared. If strong hydrophobic interactions are

present for binding the template, an aqueous two-step swelling procedure can be applied to obtain molecularly imprinted polymers in bead form (Wulff et al., 2003).

In this thesis, we prepared ion-imprinted polymer beads, which used for the selective separation of Cd^{2+} ions from human plasma. We synthesized N-methacryloyl-(L)-cysteine (MAC) as the metal complexing monomer by template polymerization, with the goal preparing a solid-phase which has the high selectivity for Cd^{2+} ions. Usually, molecularly imprinted polymers are prepared by the bulk polymerization method. The disadvantage of the method is that the obtained block polymers should be crushed, ground and sieved to produce packing materials. But in this study, Cd^{2+}-imprinted poly(hydroxyethyl methacrylate-N-methacryloyl-(L)-cysteine) beads were produced by a dispersion polymerization. PHEMA was selected as the basic polymer matrix which have hydrophilic character, good blood-compatibility properties, minimal non-specific protein interactions, high chemical and mechanical stabilities for column applications and resistance toward microbial and enzymatic attacks (Denizli et al., 1998). After removal of Cd^{2+} ions, Cd^{2+}-imprinted beads were used for the separation of cadmium from human plasma.

1.11 Magnetically Stabilized Fluidized Bed Systems (MSFB)

The separation and purification of a product from a typical biochemical reactor can require extensive capital, space and operation costs; in some cases, these recovery steps may even be the substantial fraction of the product's cost (Keller, 1983). Optimal separation processes should be versatile to reduce capital costs, able to handle large process volumes due to the dilute nature of the feed, and efficient to reduce operating costs. Additionally, the separation unit should be able to operated either batch-wise or continuously and, since a typical biochemical reactor output contains cells or cell debris, the unit should be able to handle suspended solids.

Conventional techniques for product recovery typically include a filtration or centrifugation step to remove any suspended solids followed by a batch separation operation and, if necessary, additional purification steps. The separation and purification techniques are performed predominantly in chromatography and adsorption (ion-exchange, affinity, etc.) packed columns, although for some products

liquid-liquid extraction is also feasible. Although extremely versatile, packed column separations are limited to a batch-wise operation and are not generally capable of handling cells or cell debris.

Attempts have been made to circumvent these limitations. Several separation systems operate in either a semicontinuous or continuous mode and have been developed to process aqueous feed streams (Jones, 1974; Sussman, 1976). Although these systems eliminate the problems of batch-wise operation, the presence of solids mixing in some of the devices results in uneven residence times and solids attrition. In devices where true packed columns are used (Broughton & Gembicki, 1984) complex piping/valve systems or rotary motion is necessary. These packed-column devices can perform continuous separations but are still are unable to handle solids-laden fermentation broths.

The magnetically stabilized fluidized bed (MSFB) is a continuous column separation device able to handle suspended solids. The MSFB is a fluidized bed of magnetically susceptible particles that are stabilized by a uniform magnetic field. The stabilization of the particles results in a bed that has the dispersion and mass transfer properties of a packed-bed while retaining the solids-phase fluidity of a fluidized bed. Figure 1.4 shows the stable and unstable states of the fluidized beds (Lee, 1983; Rosenweig, 1979; Siegel, 1982; Siegel, 1988).

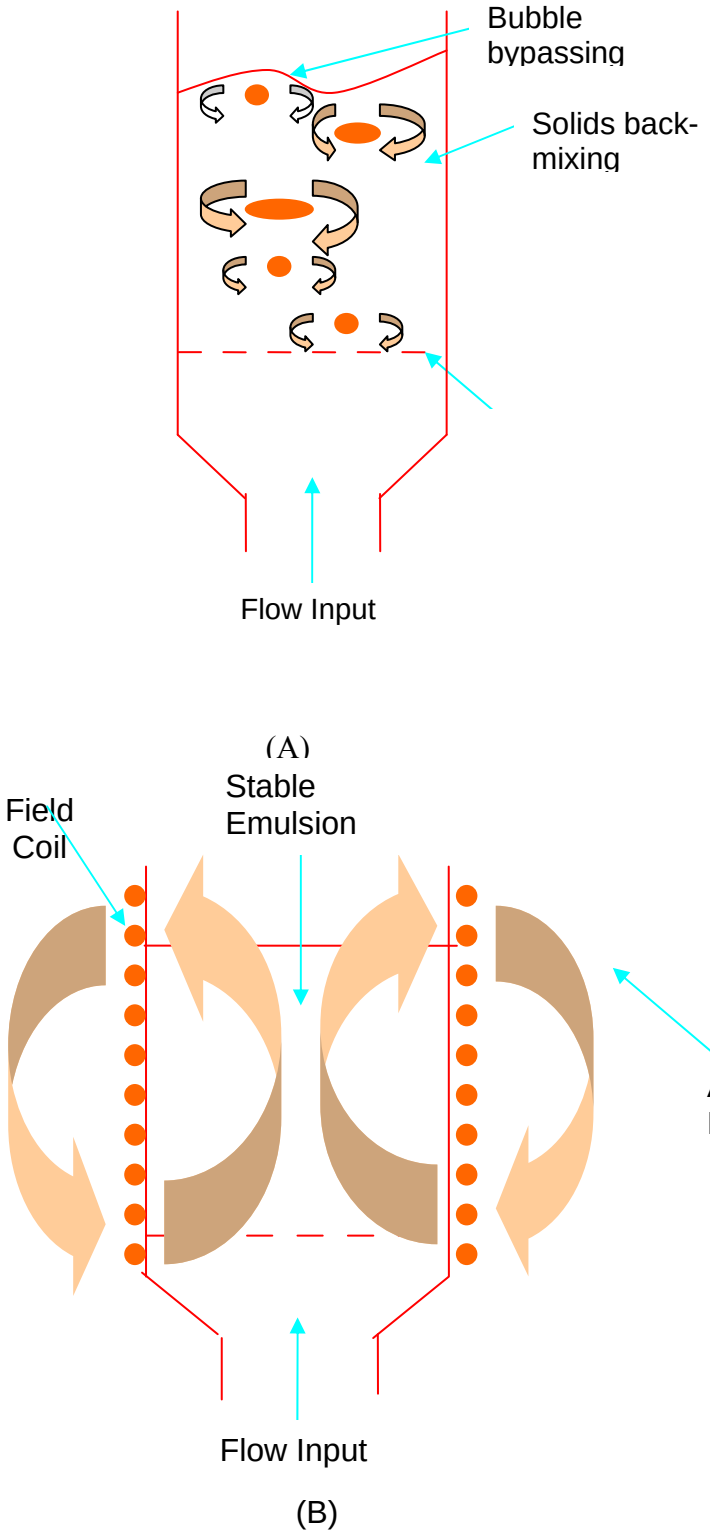

Figure 1.4 Comparison of the stable and unstable states of the fluidized beds. (A): Unstabilized, (B): Magnetically stabilized.

Other properties of the bed include little or no power consumption (if permanent magnets are used), a low and constant operating pressure drop regardless of particle size or liquid flow rate, and the ability to handle suspended solids. These properties of the bed allow continuous separation to be performed by moving both fluid phases (the liquid and the solids) countercurrent to each other. The motion of the phases is plug flow which allows many theoretical stages to be obtained in a single column. Most applications of the MSFB have involved gas fluidized beds (Albert & Tien, 1985), but more recent applications of stabilized beds can be found in biotechnology and include continuous protein recovery from aqueous streams (Burns & Graves, 1985), continuous cell filtration from fermentation broth (Terranova & Burns, 1989).

Although the liquid MSFBs used in the previously mentioned biochemical applications have many advantages over conventional techniques, they require that the support material be both magnetically susceptible and biologically active. For example, for affinity adsorption of proteins from an aqueous solution (Burns & Graves, 1985), a support was specifically designed to be both capable of binding affinity ligands and magnetically susceptible. The lack of such commercially available magnetic supports necessitates the development of special supports for each application, thereby limiting the versatility of the MSFB.

In this study, mMIP beads were prepared for the selective removal of Cd^{2+} ions from human plasma. N-methacrlyoly-(L)-cysteinemethylester (MAC) was used as the metal complexing monomer. Usually, MIPs are prepared by the bulk polymerization. The disadvantage of this method is that the obtained block polymer should be crushed, ground and sieved to obtain packing materials. Here, Cd^{2+}-imprinted poly(hydroxy ethyl methacrylate-N-methacrlyoly-(L)-cysteinemethylester) beads were prepared by suspension polymerization. After removal of Cd^{2+} ions, mMIP beads were used for the separation of Cd^{2+} ions from human plasma. Cd^{2+} adsorption and selectivity studies of cadmium versus other metal ions which are Zn^{2+} and Pb^{2+} are reported here. Finally, repeated use of the mMIP beads is also discussed.

CHAPTER TWO
EXPERIMENTAL METHODS AND MATERILAS

The monomers, 2-hydroxyethyl methacrylate (HEMA) and ethylene glycol dimethacrylate (EGDMA) were obtained from Fluka A.G. (Buchs, Switzerland), distilled under reduced pressure in the presence of hydroquinone inhibitor and stored at 4^{o}C until use. Benzoylperoxide (BPO) was obtained from Fluka (Switzerland). Poly(vinyl alcohol) (PVAL; MW: 100.000, 98% hydrolyzed) was supplied from Aldrich Chem. Co. (USA). All other chemicals were reagent grade and were purchased from Merck AG (Darmstadt, Germany). All water used in the adsorption experiments was purified using a Millipore. The resulting purified water (deionized water) has a specific conductivity of 18.2 mS.

2.1 Preparation of Polymeric Beads

2.1.1 Synthesis of N-methacryloyl-(L)-*cysteine monomer*

The following experimental procedure was applied for the synthesis of N-methacryloyl-(L)-cysteine (MAC) monomer: 5.0 g of cysteine and 0.2 g of $NaNO_2$ were dissolved in 30 mL of K_2CO_3 aqueous solution (5%, v/v). This solution was cooled to 0^{o}C. 4.0 mL of methacryloyl chloride was poured slowly into this solution under nitrogen atmosphere and then this solution was stirred magnetically at room temperature for 2 h. At the end of this period, the pH of this solution was adjusted to 7.0 and then was extracted with ethylacetate. The aqueous phase was evaporated in a rotary evaporator. The residue (i.e., MAC) was crystallized in ethanol and ethylacetate.

2.1.2 Preparation of magnetic Cd^{2+}-imprinted poly(HEMA-MAC) Beads

In the first part, MAC-Cd^{2+} complex was prepared. In order to prepare MAC-Cd^{2+} complex, solid N-methacryloyl-(L)-cysteine (MAC) (0.378 g, 2.0 mmol) was added slowly into 15 mL of ethanol and then treated with cadmium nitrate ($Cd(NO_3)_2.4H_2O$) (0.308 g, 1.0 mmol) at room temperature with continuous stirring for 3 h. Then the formed metal-comonomer complex was filtered, then washed with 99 % ethanol, and dried in a vacuum oven. 2-hydroxyethylmethacrylate (HEMA) and MAC were copolymerized in suspension by using 2,2'-azobis(izobütironitril) (AIBN) and poly(vinyl alcohol) (PVAL) as the initiator and the stabilizer, respectively. Toluene and EGDMA was included in the recipe as the diluent (as a pore former) and crosslinker, respectively.

Table 2.1 recipe and polymerization conditions for the preparation of Cd^{2+}-imprinted magnetic poly(HEMA-co-MAC) beads with a swelling ratio of 78 % and in the size range of 40-140 μm.

Table 2.1 gives the polymerization recipe and experimental conditions to obtain

Aqueous Dispersion Phase	Organic Phase
Distilled water: 50 mL	MAC-Cd^{2+} : 682 mg
	Fe_2O_3: 0.5 g
	PVAL : 0.2 g
	HEMA: 4.0 mL
	EGDMA: 8.0 mL
	Toluene: 12 mL
Polymerization Conditions	AIBN : 0.1 g
Reactor volume: 100 mL	
Stirring Rate: 600 rpm	
Temperature and Time: first at 65^{o}C for 4 h, and then at 90^{o}C for 2 h.	

Cd^{2+}-imprinted magnetic poly(HEMA-co-MAC) (mMIP) beads in the size range of 63-140 μm (in swollen form). Magnetic poly(HEMA-co-MAC) (mNIP) beads were also prepared by using the same polymerization recipe which was given in Table 2.1

only without using MAC-Cd^{2+} complex. At the end of the polymerization reaction, soluble components were removed from the polymer by repeated decantation with water and ethylalcohol. Schematic representation of polymerization system used in the preparation of Cd^{2+}-imprinted poly(HEMA-MAC) beads is shown in Figure 2.1.

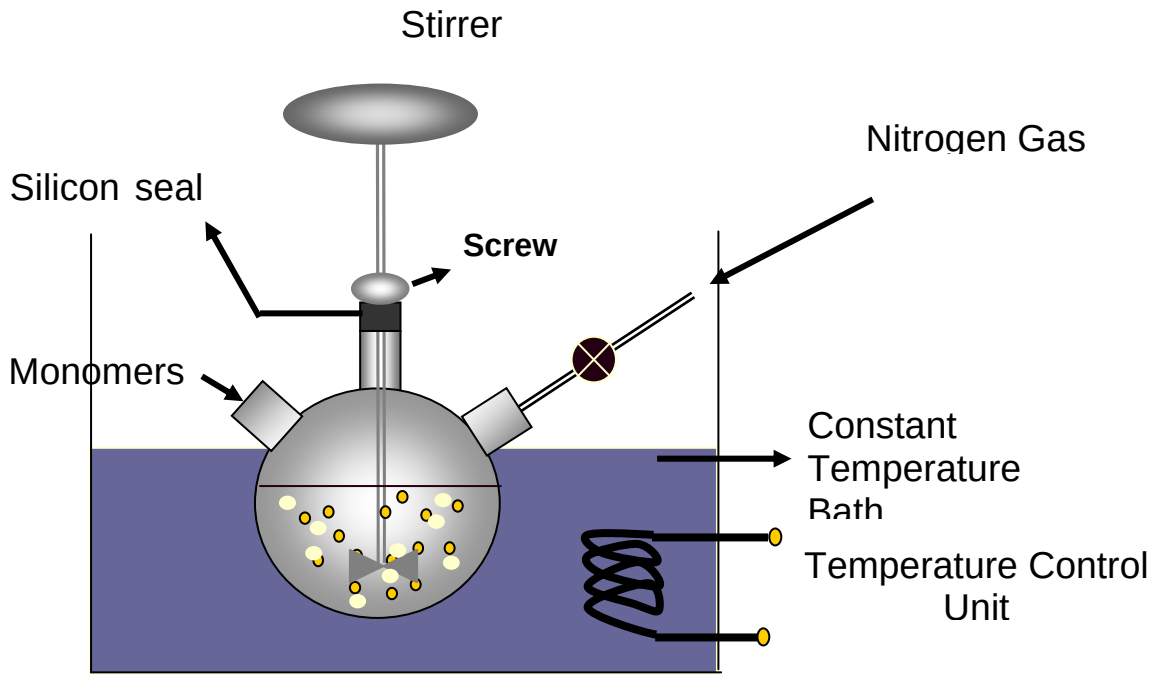

Figure 2.1 Schematic representation of polymerization system used in the preparation of Cd^{2+}-imprinted magnetic poly(HEMA-MAC) beads.

When not in use, the resulting adsorbents were kept under refrigeration in 0.02 % NaN_3 solution for preventing of microbial contamination.

2.1.3 Removal of the Template (Cd^{2+} ions)

In order to remove unreacted monomers and other ingredients the beads were extensively washed with methanol/water solution (60/40 v/v) for 24 h at room temperature. After cleaning procedure, the template was removed from the polymer beads using 0.1 M acidic thiourea. The imprinted beads were added into the 0.1 M acidic thiourea solution for 48 h at room temperature. The template free polymers

were cleaned with 0.1 M HNO_3 in a magnetic stirrer for 3 h. Cd^{2+} were found as 25.66 mg/g polymer in polymerization conditions. Cd^{2+} removal from the polymer beads were achieved as 19.166 mg per g polymer.

2.2 Characterization of Beads

2.2.1 Size Analysis

The average size and size distribution of mNIP and mMIP beads were determined by screen analysis performed by using Standard Test Sieves (Retsch GmbH & Co., Germany).

2.2.2 Surface Area Measurements

Porosity of the beads was measured by the nitrogen sorption technique, performed on Flowsorb II, (Micromeritics Instrument Corporation, Norcross, USA). The specific surface area of beads in dry state was determined by multipoint Brunauer-Emmett-Teller (BET) apparatus (Quantachrome, Nova 2200E, USA). 0.5 g of bead was placed in a sample holder and degassed in a N_2-gas stream at 150^{o}C for 1 h. Adsorption of the gas was performed at -210^{o}C and desorption was performed at room temperature. Values obtained from desorption step was used for the specific surface area calculation. The pore volume and average pore diameter were determined by BJH (Barrett, Joyner, Halenda) model on adsorption. The average size and size distribution of the beads were determined by screen analysis performed using standard sieves (Model AS200, Retsch Gmb & Co, KG, Haan, Germany).

2.2.3 Swelling Test

Water uptake ratios of mNIP and mMIP beads were determined in distilled water. The experiment was conducted as follows: initially dry beads were carefully weighed before being placed in a 50 mL vial containing distilled water. The vial was put into an isothermal water bath with a fixed temperature (25 ±0.5^{o}C) for 2 h. The bead sample was taken out from the water, wiped using a filter paper, and weighed. The

weight ratio of dry and wet samples was recorded. The water content of the poly(HEMA-MAC) and the Cd^{2+}-imprinted magnetic poly(HEMA-MAC) beads were calculated by using the following expression:

$$\text{Water uptake ratio \%} = [(W_S - W_O)/ W_O] \times 100 \qquad (2.1)$$

Where W_O and W_S are the weights of beads before and after uptake of water, respectively.

2.2.4 Surface Morphology

The surface morphology of the polymeric beads was examined using scanning electron microscopy (SEM). The samples were initially dried in air at 25°C for seven days before being analyzed. A fragment of the dried bead was mounted on a SEM sample mount and was sputter coated for 2 minutes. The sample was then mounted in a scanning electron microscope (Model: Raster Electronen Microscopy, Leitz-AMR-1000, Germany). The surface of the sample was then scanned at the desired magnification to study the morphology of mNIP and mMIP beads.

2.2.5 Elemental Analysis

To evaluate the degree of MAC incorporation mNIP and mMIP beads were subjected to elemental analysis using a Leco Elemental Analyzer (Model CHNS-932).

2.2.6 FTIR Studies

FTIR spectra of MAC and mMIP beads were obtained by using a FTIR spectrophotometer (FTIR 8000 Series, Varian). The dry beads (about 0.1 g) was thoroughly mixed with KBr (0.1 g, IR Grade, Merck, Germany), and pressed into a pellet and the FTIR spectrum was then recorded.

2.2.7 Analysis of Magnetizm

The magnetism degree of the mMIP microbeads was measured in a magnetic field by using a vibrating-sample magnetometer (Princeton Applied Research, USA). The presence of magnetite particles in the polymeric structure was investigated with electron spin resonance (ESR) spectrophotometer (EL 9, Variant).

2.3 Adsorption-Desorption Studies

2.3.1 Adsorption of Cd^{2+} Ions From Aqueous Solutions

Adsorption of Cd^{2+} ions from aqueous solutions on the mNIP and mMIP beads was studied in batch-wise. After the desired treatment periods Cd^{2+} ions was measured by using an atomic absorption spectrophotometer. A hollow cathode cadmium lamp was used. The working wavelength and detection limit was 228.8 nm and 0.028 ppm. The instrument response was periodically checked with known Cd^{2+} solution standards. The experiments were performed in replicates of three and the samples were analyzed in replicates of three as well. For each set of data present, standard statistical methods were used to determine the mean values and standard deviations. Confidence intervals of 95% were calculated for each set of samples in order to determine the margin of error. The amount of Cd^{2+} adsorption per unit mass of the beads was evaluated by using the following expression:

$$Q = [(C_O - C) . V] / m \quad (2.2)$$

Here, Q is the amount of Cd^{2+} ions adsorbed onto unit mass of the beads (μmol/g); C_O and C are the concentrations of the Cd^{2+} ions in the initial solution and in the aqueous phase after treatment for certain period of time, respectively (μmol/L); V is the volume of the solution (L); and m is the mass of the beads used (g). For adsorption-desorption studies with Cd(II) adsorption from aqueous solutions onto the mMIP microbeads; pH effect in the range of at 4-8, adsorption capacity from 5 ppm to 100 ppm Cd^{2+} and time dependence for 120 minutes were investigated.

2.3.2 Selectivity Experiments

In order to show Cd^{2+} specificity of mMIP beads, competitive adsorptions (i.e., lead (Pb^{2+}; Mw: 207.2 g/mol, ionic radius: 133 pm and zinc (Zn^{2+}; Mw=65.39 g/mol, ionic radius: 88 pm) were also studied. The mMIP beads were treated with this competitive ions. After adsorption equilibrium, the concentration of Pb^{2+} and Zn^{2+} ions in the remaining solution was measured by AAS. The working wavelengths were 283.3, 213.9 nm and detection limits were 0.450, 0.018 ppm for Pb and Zn. Distribution and selectivity coefficients of Pb^{2+} and Zn^{2+} with respect to Cd^{2+} were calculated as explained by the following Equation (2.3)

$$K_d = [(C_i - C_f)/C_f] \times V/m \qquad (2.3)$$

Here, K_d represents the distribution coefficient; C_i and C_f are initial and final concentrations of metal ions, respectively. V is the volume of the solution (mL) and m is the mass of beads used (g).

The selectivity coefficient for the binding of a metal ion in the presence of competitor species (Eq. 2.4) can be obtained from equilibrium binding data according to (Eq. 2.5).

$$M_1(\text{solution}) + M_2(\text{sorbent}) <=> M_2(\text{solution}) + M_1(\text{sorbent}) \qquad (2.4)$$

$$K = ([M_2]\text{solution}\ [M_2]\text{sorbent}) / ([M_1]\text{solution}\ [M_2]\text{sorbent}) \qquad (2.5)$$

$$k = K_d(Cd^{2+}) / (K_d(X^{2+})$$

where k is the selectivity coefficient and X^{2+} represents Pb^{2+} and Zn^{2+} ions. A comparison of the k values of the imprinted beads with those metal ions allows an estimation of the effect of imprinting on selectivity.

A relative selectivity coefficient k` (eq. 2.6) can be defined as

$$k` = k_{imprinted}/k_{control} \qquad (2.6)$$

2.4 Desorption and Repeated Use

Desorption of Cd^{2+} ions were studied with two different desorption agent; 0.1 M acidic thiourea (NH_2SHNH_2) solution, 0.1 M nitric acid (HNO_3) solution, respectively. The mMIP beads were placed in this desorption medium and stirred continuously (at a stirring rate of 400 rpm) for 1 h at room temperature. The final Cd^{2+} ions concentration in the desorption medium was measured by atomic adsorption spectrometer. The desorption ratio was calculated from the amount of Cd^{2+} ions adsorbed on the beads and the final Cd^{2+} ions concentration in the desorption medium by the following equation (2.7.)

$$\text{Desorption Ratio} = \frac{\text{amount of } Cd^{2+} \text{ ions desorbed to the elution medium}}{\text{amount of } Cd^{2+} \text{ ions adsorbed on the beads}} \text{ x100}$$

In order to test the reusability of mMIP beads Cd^{2+} ions adsorption-desorption procedure was repeated ten times by using the same polymeric sorbent. In order to regenerate and sterilize, after desorption; the beads were washed with 50 mM NaOH solution.

2.5 Adsorption of Cd^{2+} Ions From Human Plasma

Adsorption of Cd^{2+} ions from human plasma on mNIP and mMIP beads were carried out in a magnetically stabilized fluidized bed. Human blood is collected from thoroughly controlled voluntary blood donors. No preservatives are added to the samples. Human blood was collected into EDTA-containing vacutainers and red blood cells were separated from plasma by centrifugation at 4000 g for 30 min at room temperature, then filtered (3 μm Sartorius filter) and frozen at -20^{o}C. Before use, the plasma was thawed for 1 h at 37^{o}C. Nitrate salt was used as the source of Cd^{2+} ions. The beads suspended in pure water were degassed under reduced pressure (by using water suction pump) and magnetically stabilized into a column (10 cm x 0.9 cm inside diameter) equipped with a water jacket for temperature control. The vertically oriented magnetic field was produced by passing DC current through two modified Helmholtz coils (1.5 cm diameter x 2.5 cm thick) spaced 4 cm apart. At a current of 1.6 A (50 W), each coil produced a magnetic field of 40 Gauss. Equilibration of the column was performed by passing four column volumes of phosphate buffer (pH: 7.4) before injection of the overdosed. Then, 20 ml of the overdosed human plasma was passed through the column containing beads, by a peristaltic pump for 2 h. Dynamic binding capacity (DBC) was calculated from Cd^{2+} ions breakthrough curves.

CHAPTER THREE

RESULTS AND DISCUSSIONS

3.1 Characterization of mMIP Beads

mMIP beads were synthesized by suspension polymerization. The fraction size of the beads were fall in the range of 63-140 μm were used throughout the study. The size range of mNIP beads is similar to that of mMIP beads size. Specific surface area, total pore volume and average pore diameter of the mNIP and the mMIP beads are presented in Table 3.1. The specific surface area of the mMIP beads was found to be 24.7 m^2/g polymer by the multipoint BET measurements. According to the BJH method, the pore diameter of the mMIP beads changed between 20 and 300 Å and average pore diameter is 32.0 Å. This indicated that the mMIP beads contained mainly mesopores.

Table 3.1 Physical properties of mNIP and mMIP beads.

Polymer	Surface Area[a] (m^2/g)	Total Pore Volume[b] (ml/g)	Average Pore Diameter[c] (Å)
mNIP	20.3	0.044	26.8
mMIP	24.7	0.061	32.0

a. Determined using multipoint BET method

b BJH cumulative desorption pore volume of pores between 20 and 245 Å

c. BJH desorption average pore diameter of pores between 20 and 245

Screen analysis of the synthesized mMIP microbeads was performed with Retsch standard sieves. Figure 3.1. shows the size-size distribution of the mMIP microbeads obtained with the polymerization recipe given in Table 2.1.

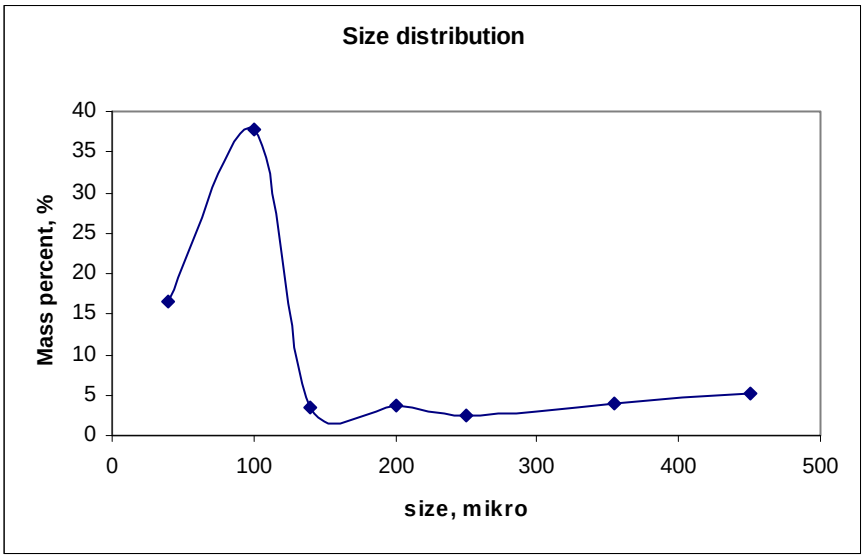

Figure 3.1 Size distribution of Cd^{2+}imprinted magnetic poly(HEMA-MAC) beads.

The surface morphology and bulk structure of the mMIP beads are exemplified by the electron micrographs in Figure 3.2. All the beads have a spherical form and rough surface. In the SEM photograph of the bulk structure, a large quantity of well-distributed pores could be observed and they were netlike. It is well known that, in order to facilitate the transfer of metal ions, the gel beads should have large pores (i.e., mesopores). The mMIP beads prepared in this study had this characteristics and these mesopores would increase the specific surface area, the adsorption capacity of mMIP beads, as well as the mass transfer rate of releasing and rebinding template metal ions. It is clearly seen also that the mMIP beads were more porous than the corresponding mNIP beads.

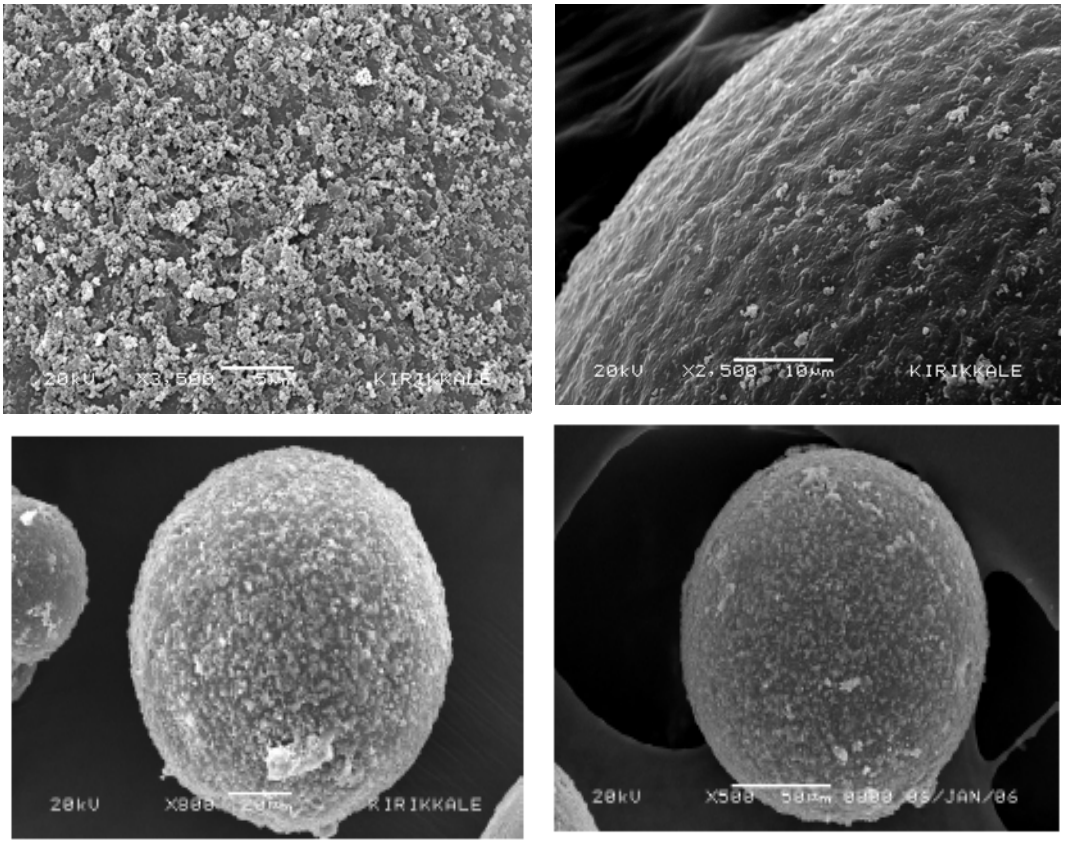

MIP NIP

Figure 3.2. SEM micrographs of Cd^{2+}-imprinted magnetic p(HEMA-MAC) beads:

The equilibrium swelling ratios of the mNIP and mMIP beads are 63% and 70%, respectively. Formation of metal ion imprinted cavities in the polymer structure introduced more hydrodynamic volume into the polymer chains, which can result uptake in the more water molecules by ion-imprinted polymer matrix. The incorporation of the MAC was found to be 41.8 µmol/g polymer by using nitrogen stoichiometry. Note that HEMA and other polymerization ingredients do not contain nitrogen. This nitrogen amount determined by elemental analysis comes from only incorporated MAC groups into the polymeric structure. N-methacryloyl-(L)-cysteine (MAC) was selected as the comonomer and ionimprinted monomer for the selective separation of Cd^{2+} ions from human plasma. In the first step, MAC was synthesized

from cysteine and methacryloyl chloride and complexed with Cd^{2+} ions. The molecular formula of synthesized MAC comonomer and MAC-Cd^{2+} complex are shown in Figure 3.3. FTIR spectrum of MAC has the characteristic stretching vibration amide I and amide II absorption bands at 1651 cm^{-1} and 1558 cm^{-1}, carbonyl band at 1724 cm^{-1}. For the characteristic determination of complex, due to linear coordinate covalent complex formation, the characteristic strong S-H stretching vibration bands at 1130 cm^{-1} and 970 cm^{-1} slips to the higher frequency field at 950 cm^{-1} and 750 cm^{-1}, (show on FTIR spectrum as indicated in red arrow) as a result of decreasing the electron density of sulfhydryl group of MAC monomer (Figure 3.4a). Then, MAC-Cd^{2+} complex was polymerized with HEMA comonomer by suspension polymerization technique. The FTIR spectrum of mMIP beads has the characteristic stretching vibration band of hydrogen bonded alcohol, O-H, around 3444 cm^{-1}, carbonyl at 1731 cm^{-1} amide II absorption bands at 1455 cm^{-1}, respectively (Figure 3.4b).

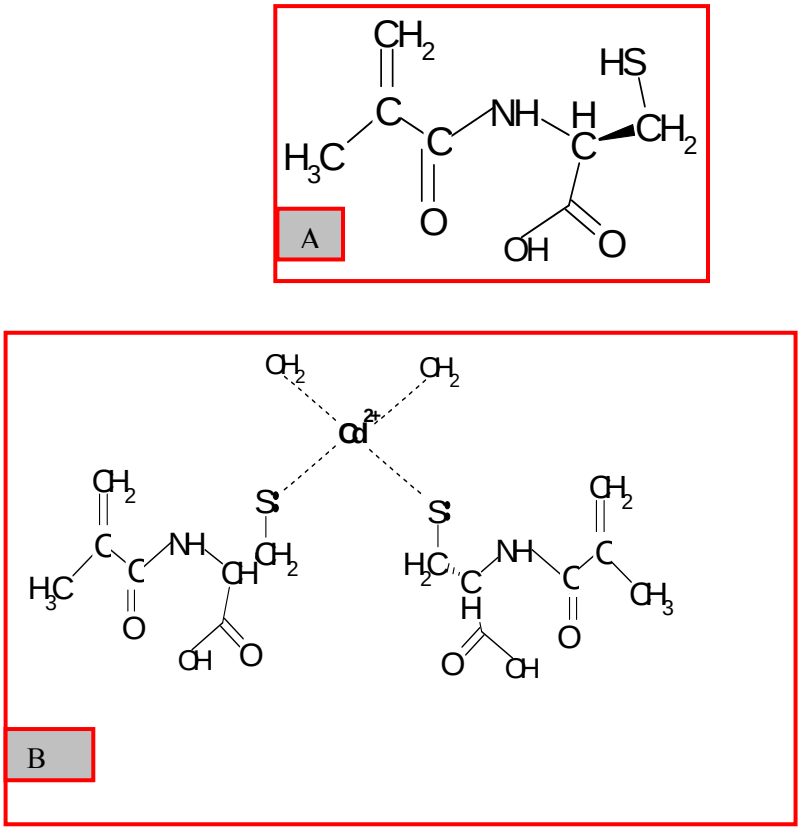

Figure 3.3. The molecular formula of (A) MAC monomer (B) mMIP beads

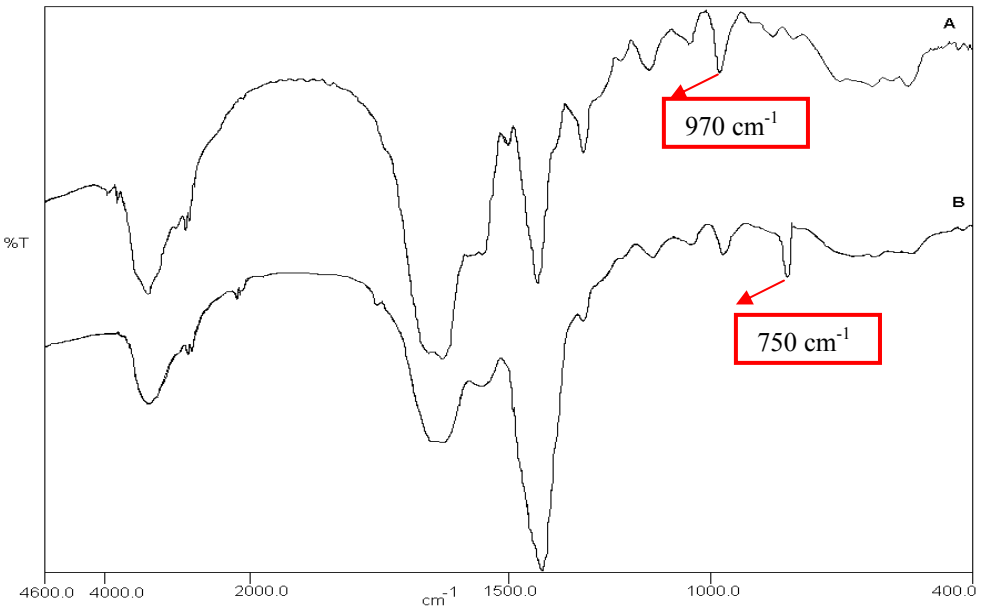

Figure 3.4 a FTIR spectrum of MAC (B) and MAC-Cd^{2+} monomer (A).

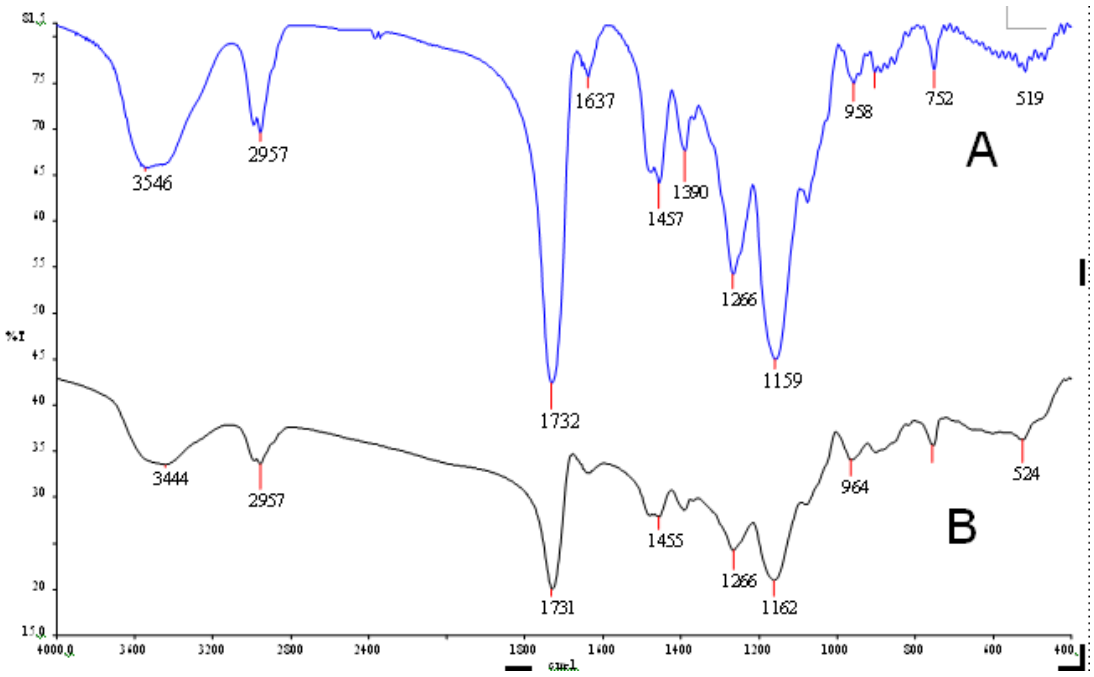

Figure 3.4 b FTIR spectrum of mNIP polymer (A) and mMIP (B).

The FTIR spectra of mNIP and mMIP beads have the characteristic stretching vibration band of hydrogen bonded alcohol, O-H, around 3500 cm^{-1}, carbonyl around 1730 cm^{-1}, amide I and amide II absorption bands around 1630 cm^{-1} and 1450cm^{-1}, respectively (Fig. 3.4b). Note that both mNIP and mMIP beads were polymerized in the same conditions.

Magnetic characteristics of magnetic materials are related to their sorts generally, while those of magnetic materials are usually related to content of magnetic component inside. So, Fe_3O_4 content is very important to the magnetic responsibility of magnetic materials. In general, the higher Fe_3O_4 content shows the stronger magnetic responsibility (Lu et al., 2006). For this reason, the average Fe_3O_4 content of the mMIP beads was determined by density analysis. The hydrated density of the mMIP beads measured at 25°C was 1.19 g/mL. By the same procedure, the density of Fe_3O_4 particles was found to be 1.97 g/mL at 25°C. The density of non-magnetic MIP beads measured at 25°C was 1.12 g/mL. The magnetic particles volume fraction in the mMIP beads can be calculated from the following equation derived from the mass balance:

$$\phi = (\rho_C - \rho_M) / (\rho_C - \rho_A)$$

where, ρA, ρC and ρM are the densities of non-magnetic MIP beads, Fe_3O_4 nanopowder, and the mMIP beads, respectively. Thus with the density data mentioned above, the mMIP beads gel volume fraction in the magnetic beads was estimated to be 91.8 %. Therefore, the average Fe_3O_4 content of the resulting mMIP beads was 8.2 %. Magnetite (Fe_3O_4) is a biocompatible superparamagnetic material that has low toxicity and strong magnetic properties (Huang et al., 2003). However, the leach of magnetite nanopowder was measured in three different kinds of media including acetic acid solution (50%, v/v, pH: 2.0), phosphate buffer solution (pH: 7.0) and sodium citrate/NaOH buffer solution (pH: 12.0). It should be noted that there was no measurable release. The presence of magnetite nanopowder in the polymer structure was also confirmed by the ESR. The intensity of the magnetite peak against magnetic field (Gauss) is shown in Figure 3.5. A peak of magnetite was detected in the ESR spectrum. It should be noted that the nonmagnetic MIP beads can not be magnetized under this condition. It reflects response ability of magnetic materials to the change of external magnetic field firstly and it characterizes ability of magnetic materials to keep magnetic field strength when external magnetic field being removed. In order to show magnetic stability, the mMIP beads were kept in distilled water and ambient air for 3 months, and the same ESR spectra was obtained. With the goal of testing the mechanical stability of the mMIP beads, a bead sample

was treated in a ball mill for 2 h. SEM photographs show that a zero percentage of the sample was broken.

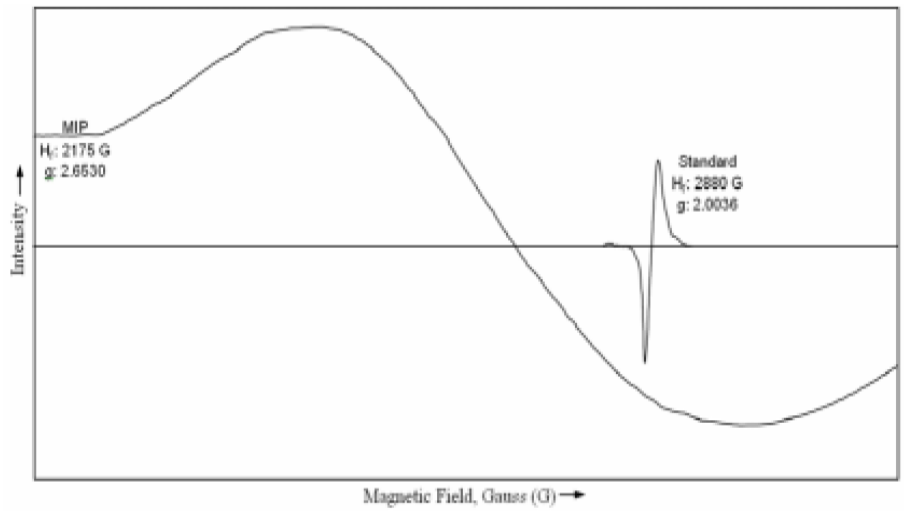

Figure 3.5 ESR spectrum of mMIP beads.

The g factor given in Figure 3.5 can be considered as quantity characteristic of the molecules in which the unpaired electrons are located, and it is calculated from Eq. 6. The measurement of the g factor for an unknown signal can be a valuable aid in the identification of a signal. In the literature the g factor for Fe^{+3} is determined between 1.4-3.1 for low spin and 2.0-9.7 for high spin complexes (Swartz et al., 1972). In this study, the g factor was found to be 2.65 for mMIP structure.

$g = h.\nu / \beta. Hr$ (6)

Here, h is the Planck constant (6.626 x 10-27 erg/s); β is Universal constant (9.274 x 10-21 erg/G); ν is frequency (9.707 x 109 Hz) and Hr is resonance of magnetic field (G).

Magnetic properties of polymeric structure was also shown using electron mass unit (EMU), showing the behaviour of magnetic beads in a magnetic field using a vibrating magnetometer, in Figure 3.6, and Hr value, is defined as the external magnetic field at resonance. In EMU spectrum and from Hr value, 2175 Gauss magnetic field was found sufficient to excite all of the dipole moments present in 1.0 g of mMIP sample. This value will be an important design parameter for a magnetically stabilized fluidized bed or magnetic filtration using the mMIP beads.

The value of this magnetic field is a function of the flow velocity, bead size and magnetic susceptibility of solids to be removed. In the literature, this value was found to change from 8 kG to 20 kG for various applications, thus magnetic beads presented in this study will need less magnetic intensity in a magnetically stabilized fluidized bed or for a magnetic filter system (Özkara et al., 2004).

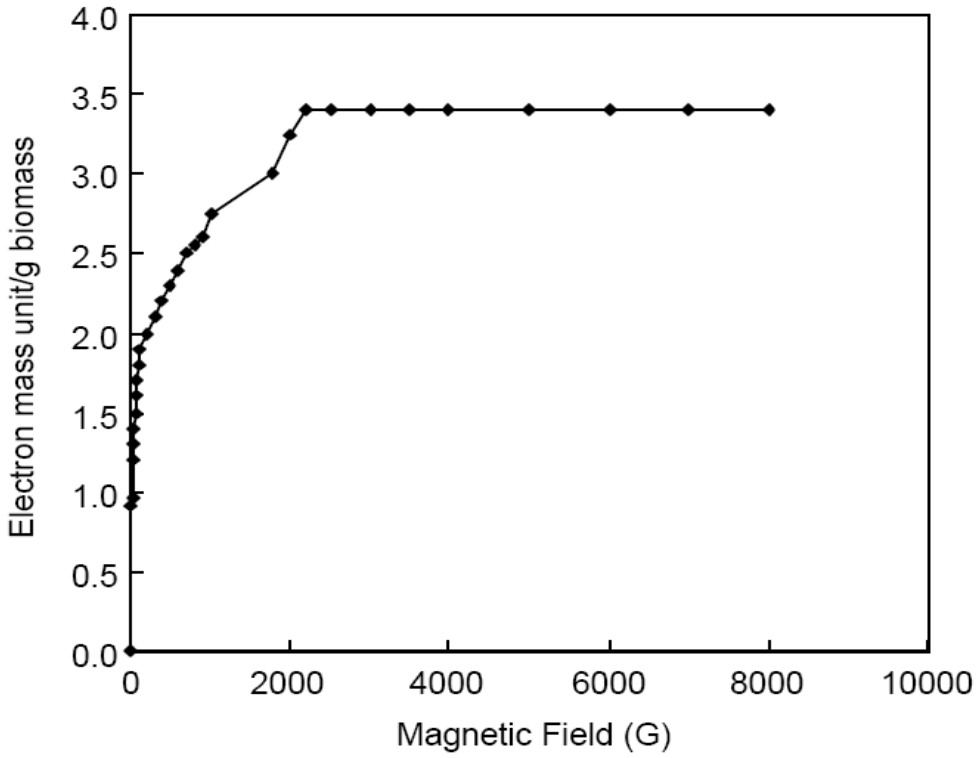

Figure 3.6 The magnetic behavior of mMIP beads.

3.2 Adsorption-Desorption Studies from From Aqueous Solutions Batch-wise

3.2.1 pH Effect on the Cd^{2+} Adsorption

In order to establish the effect of pH on adsorption of Cd^{2+} ions onto mMIP and mNIP beads, we repeated the batch adsorption equilibrium studies at different pHs in the range 4.0-8.0. Figure 3.7 shows that cadmium (II) adsorption by the mMIP beads was low at pH 4.0, but increased rapidly with increasing pH and reached the maximum at pH 7.4 as 23.75 μmol per gram dry weight of beads. Then, decreased rapidly at pH 8.0.

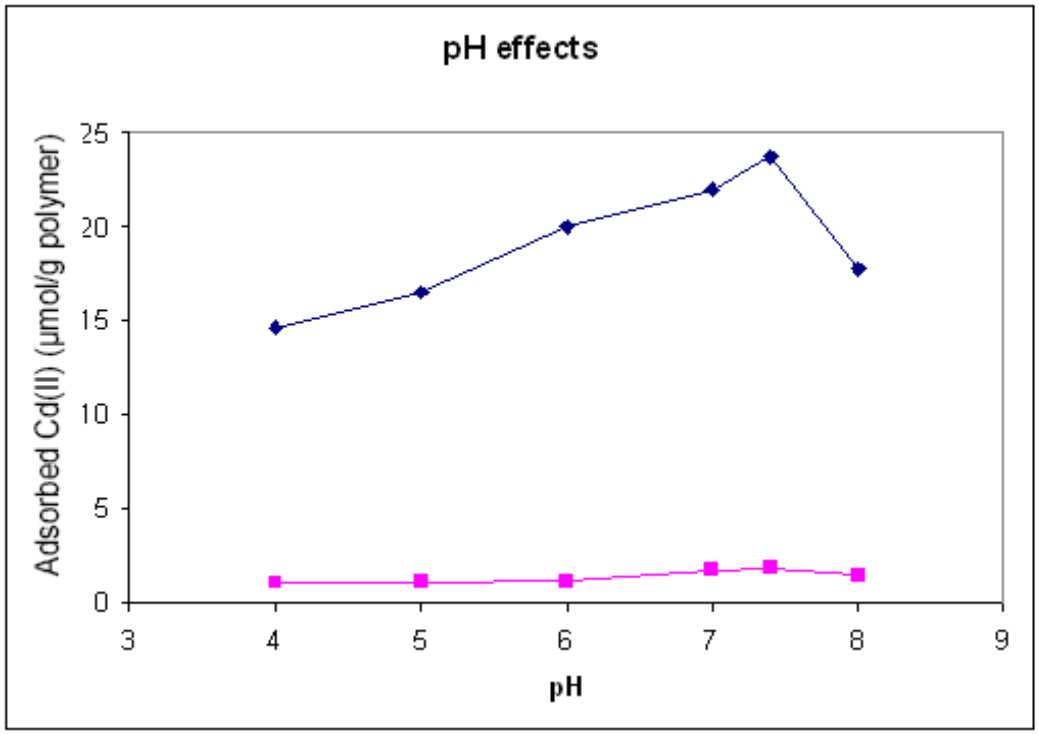

Figure 3.7. Effect of pH on adsorbtion of Cd^{2+} ions on mMIP beads , -♦- and mNIP beads, -■- V_{total}:10 mL, 25 mg/L solution, 25 mg polymer, time: 60 min and T:25°C.

3.2.2 Effect of Time

Figure 3.8 shows the time dependence of the adsorption values of Cd^{2+} ions on mNIP and mMIP beads. The adsorption rate was relatively very fast, the time required to reach equilibrium conditions was about 60 min. The maximum adsorption capacity for Cd^{2+} ions was 28.45 µmol per gram dry weight of beads.

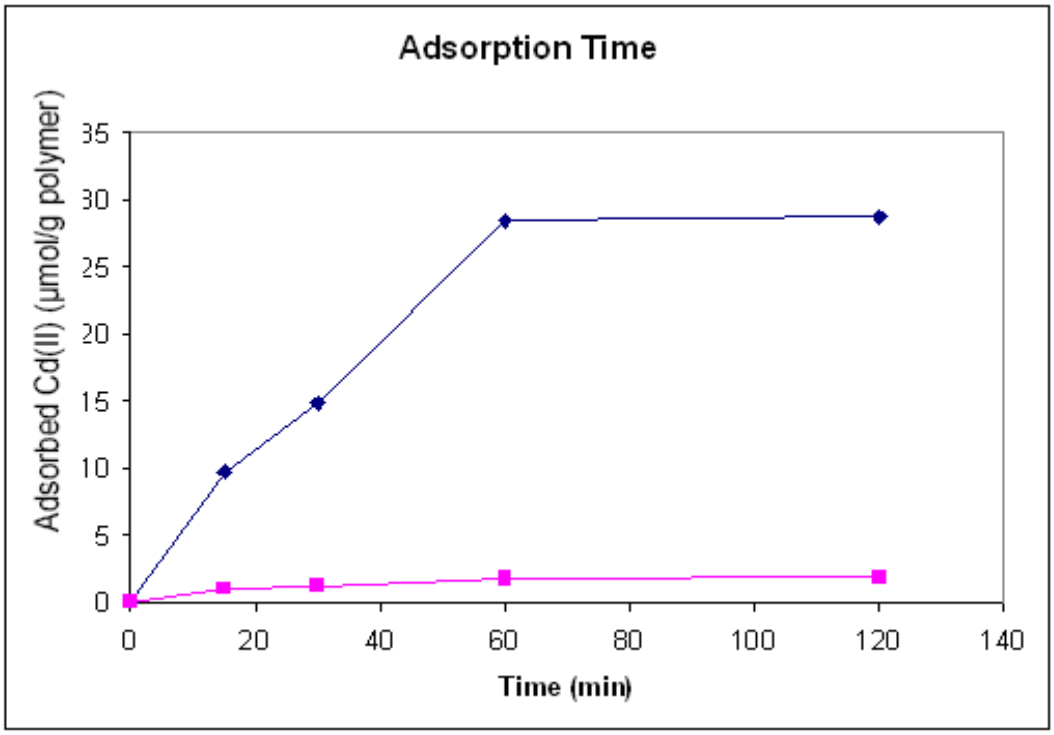

Figure 3.8. Time dependent adsorption of Cd^{2+} ions on mMIP beads, -♦- and mNIP beads, -■-: Initial concentrarion of metal ions: 40 mg/L solution, Vtotal: 10 mL, 25 mg polymer and T: 25°C.

3.2.3 Effect of Initial Concentration of Cd^{2+} ions

Figure 3.9 shows the equilibrium concentration of metal ions dependence of the adsorbed amount of the Cd^{2+} onto mMIP and mNIP beads. The adsorption values increased with increasing concentration of Cd^{2+} ions, and a saturation value is achieved at ion concentration of 60 mg/L as 28.45 μmol/g polymer as maximum adsorption capacity, which represents saturation of the active binding cavities on the mMIP beads.

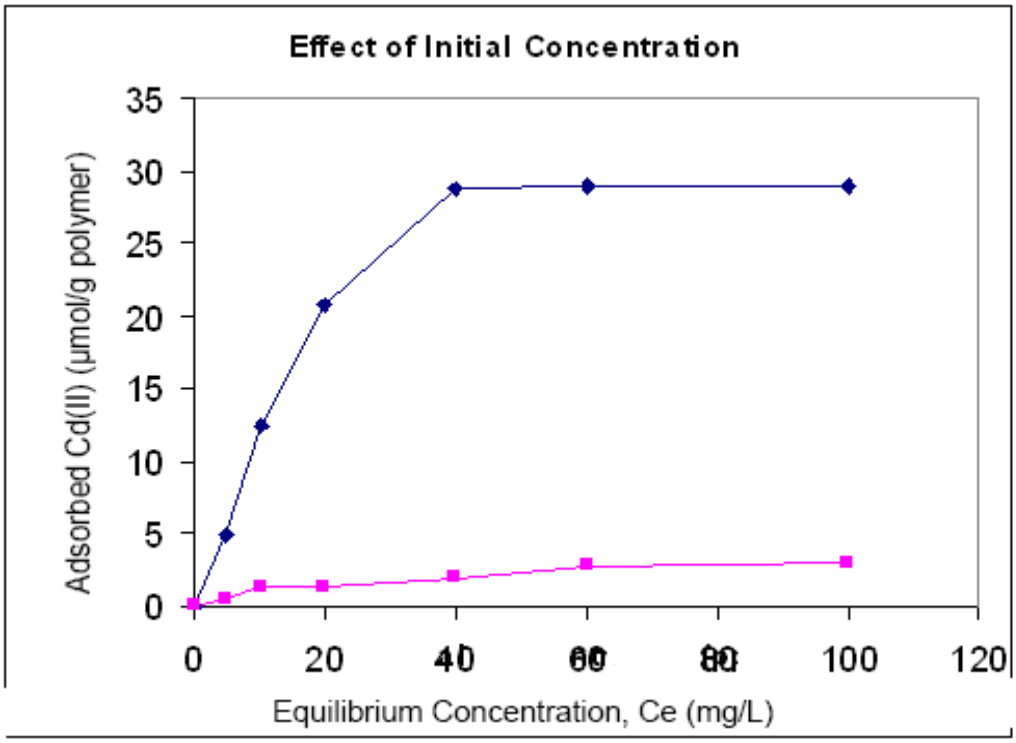

Figure 3.9. Effect of initial Cd^{2+} concentration on adsorption of mMIP beads, -♦- and mNIP beads, -■ -: pH 7.4; Vtotal: 10 mL; 25 mg polymer, time: 60 min, T: 25°C.

3.3 Langmuir Adsorption Model

An adsorption isotherm is used to characterize the interactions of each molecules with the adsorbents. This provides a relationship between the concentration of the molecules in the solution and the amount of ion adsorbed on the solid phase when the two phases are at equilibrium. The Langmuir adsorption model assumes that the molecules are adsorbed at a fixed number of well-defined sites, each of which is capable of holding only one molecule. These sites are also assumed to be energetically equivalent, and distant from each other so that there are no interactions between molecules adsorbed on adjacent sites.

During the batch experiments, adsorption isotherms were used to evaluate adsorption properties. The Langmuir adsorption isotherm is expressed by Equation 3.1. The corresponding transformations of the equilibrium data for Cd^{2+} ions gave rise to a linear plot, indicating that the Langmuir model could be applied in these systems and described by the equation:

$$Q = Q_{max}.\ b\ .\ C_{eq}/\ (1+bC_{eq}) \qquad (3.1)$$

where Q is the concentration of bound Cd^{2+} ions in the adsorbent (μmol/g), Ceq is the equilibrium Cd^{2+} ions concentration in solution (μmol /L), b is the Langmuir constant (g/μmol) and, Q_{max} is the adsorption capacity (μmol/g). This equation can be linearized so that

$$1/Q = [1/(Q_{max}.\ b)][\ 1/C_{eq}] + [1/(Q_{max}.] \qquad (3.2)$$

The plot of $1/C_{eq}$ versus 1/Q was employed to generate the intercept of 1/Qmax and the slope of $1/Q_{max}.b$ (Figure 3.10).

Freundlich model;

$lnq_e = LnK_f + 1/n \ln Ce$

q_e – mg metal ion adsorbed / g adsorbent

Ce – mg /dm^3

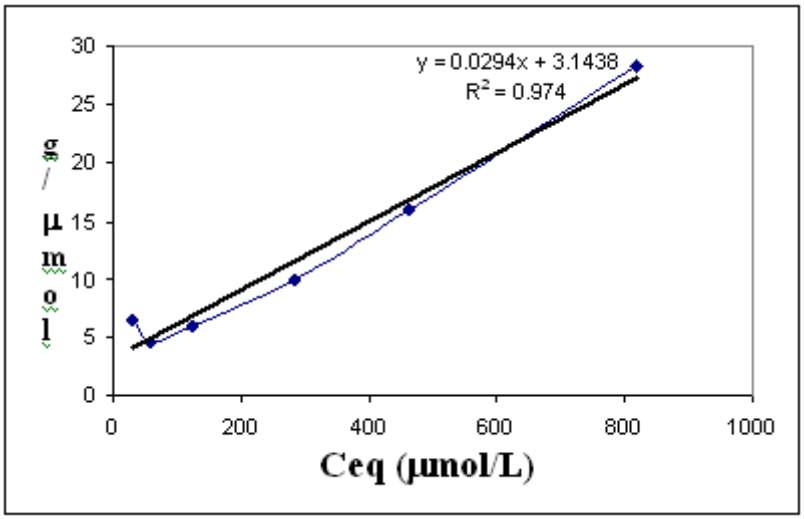

Figure 3.10. Langmuir adsorption isotherm. Cd^{2+} ions concentration 40 mg/L; pH: 7.4; T: 25°C for mMIP.

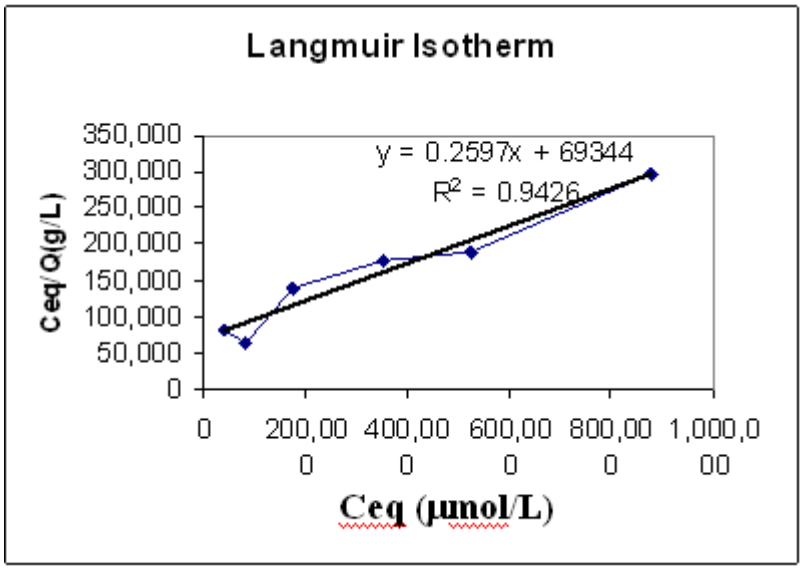

Figure 3.11 Lagmiur adsorption isotherm for mNIP.

The maximum adsorption capacity (Q_{max}) data for the adsorption of Cd^{2+} ions on the imprinted polymer was obtained from the experimental data. The correlation coefficients (R^2) were 0.974 at pH 7.4. The Langmuir adsorption model can be applied in this affinity adsorbent system. It should be also noted that the maximum adsorption capacities (Q_{max}) and the Langmuir constants were found to be 34.01 µmol/g (pH 7.4) and 9.35 10^{-3} g/µmol, respectively (Fig.3.10). For non-imprinted polymer the correlation coefficients (R^2) were 0.9426 at pH 7.4. The Langmuir

adsorption model the maximum adsorption capacities (Q_{max}) and the Langmuir constants were found to be 3.8505 μmol/g (pH 7.4) and 3.74 x 10^{-6} g/μmol, respectively for non-imprinted polymer (Fig. 3.11).

In order to examine the controlling mechanism of adsorption process such as mass transfer and chemical reaction, kinetic models were used to test experimental data. The kinetic models (Pseudo-first and second-order equations) can be used in this case assuming that the measured concentrations are equal to adsorbent surface concentrations. The first-order rate equation of Lagergren is one of the most widely used for the adsorption of solute from a liquid solution (Cheung et al., 2001). It may be represented as follows:

$dq_t/dt=k_1(q_{eq}-q_t)$ (3.3)

where k_1 is the rate constant of pseudo-first order adsorption (min^{-1}) and q_{eq} and q_t denote the amounts of adsorbed protein at equilibrium and at time t (μmol/g), respectively. After integration by appliying boundary conditions, $q_t=0$ at t=0 and $q_t=q_t$ at t=t, gives

$\log[q_{eq}/(q_{eq}-q_t)]= (k_1t)/2.303$ (3.4)

Equation 4.4 can be rearranged to obtain a linear form

$\log(q_{eq}-q_t)= \log(q_{eq}) - (k_1t)/2.303$ (3.5)

a plot of $\log(q_{eq})$ versus t should give a straight line to confirm the applicability of the kinetic model. In a true first-order process $\log q_{eq}$ should be equal to the interception point of a plot of $\log(q_{eq}-q_t)$ via t.

In addition, a pseudo-second order equation based on adsorption equilibrium capacity may be expressed in the form (Yuh-Shan Ho, 2006),

$dq_t/dt = k_2 (q_{eq}-q_t)^2$ (3.6)

Where k_2 (g μmol^{-1} min^{-1}) is the rate constant of pseudo-first order adsorption process. Integrating equation 4.6, q and applying the boundary conditions, $q_t=0$ at t=0 and $q_t=q_t$ at t=t, leads to

$1/(q_{eq}-q_t)] = (1/q_{eq}) + k_2t$ (3.7)

or equivalently for linear form

$(t/q_t)= (1/k_2q_{eq}^2) + (1/q_{eq})\, t$ (3.8)

a plot of t/q_t versus t should give a linear relationship for the applicability of the second-order kinetics. The rate constant (k_2) and adsorption at equilibrium (q_{eq}) can be obtained from the intercept and slope, respectively (Table 3.2).

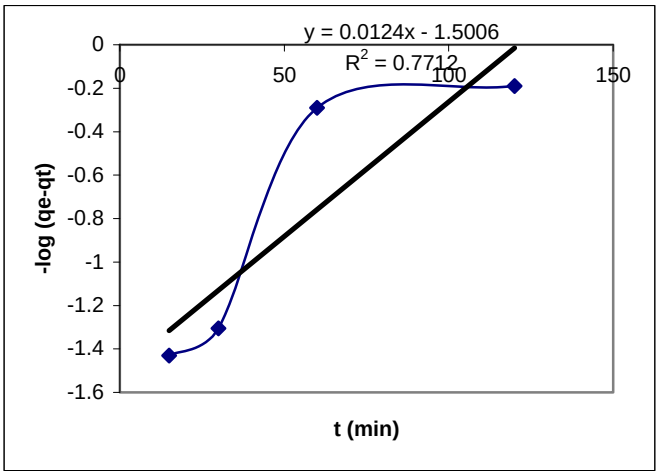

Figure 3.12. Pseudo-first-order kinetic of the experimental data for mMIP

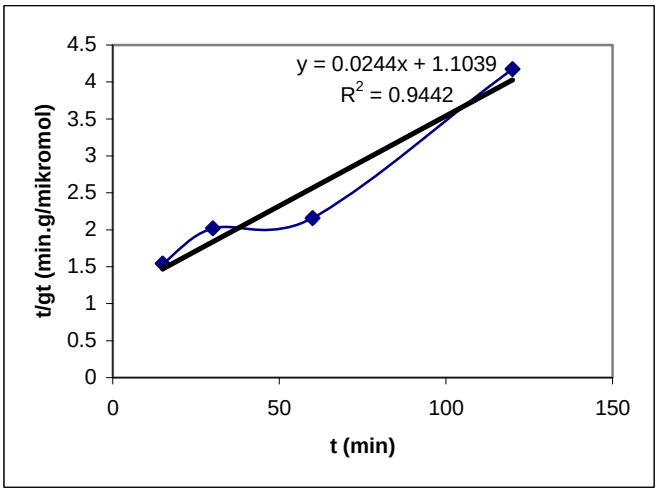

Figure 3.13. Pseudo-second-order kinetic of the experimental data for mMIP

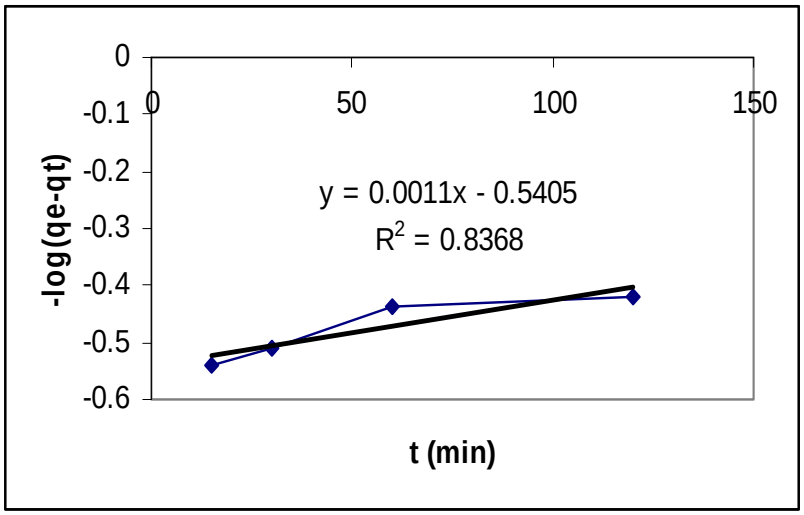

Figure 3. 14. Pseudo-first-order kinetic of the experimental data for the mNIP.

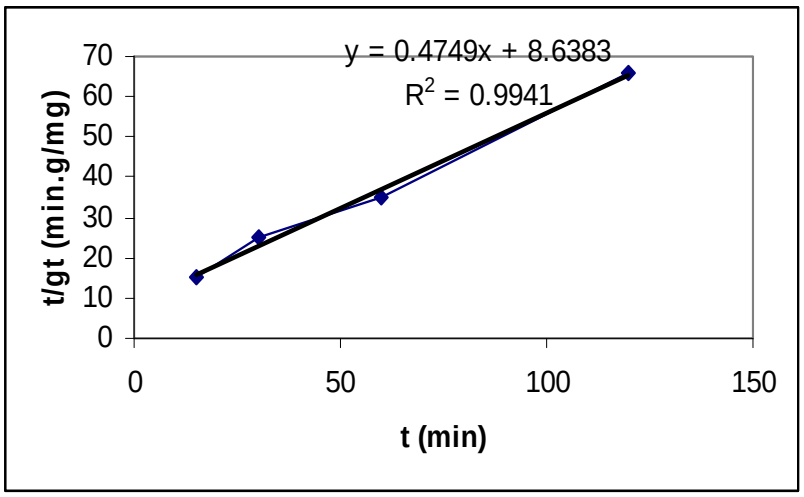

Figure 3.15. Pseudo-second-order kinetic of the experimental data for mNIP.

Table 3.2 Kinetic constants for the mMIP and mNIP beads.

Initial Conc. (mg/L)	Experimental	First-order kinetic			Second-order kinetic		
		slope	*intercept*		*intercept*	*slope*	
40	Qeq (μmol/g)	k_1 (1/min)	q_{eq} (μmol /g)	R^2	k_2 (g/μmol.min)	q_{eq} (μmol /g)	R^2
MIP	28.94	2.8×10^{-2}	31.66	0.77	5.3×10^{-4}	40.98	0.94
NIP	2.95	2.5×10^{-3}	3.47	0.83	2.6×10^{-2}	2.10	0.99

3.4 Selectivity Experiments

Adsorption capaties of the mMIP beads for metal ions under competitive conditions (i.e. adsorption from solutions containing 10 mg/l from each of Cd (II), Zn(II) adn Pb(II) ions) are given Table 3.3. Pb^{2+} and Zn^{2+} were chosen as competitive metal ions because of their similar ionic radius. Competitive adsorption of Pb^{2+}/Cd^{2+} and Zn^{2+}/Cd^{2+} from their mixtures were also studied in a batch system. Table 3.3 and Fig. 3.16 summarizes K_d, and k, values of Pb^{2+} and Zn^{2+} with respect to Cd^{2+}.

Table 3.3. K_d (ml/g), k, and values of Pb^{2+} and Zn^{2+} with respect to Cd^{2+}.

Metal ions	mNIP		mMIP		
	Kd	k	Kd	k	k^I
Cd^{2+}	6.90	-	297.2		
Pb^{2+}	10.26	0.67	15.40	19.20	28.65
Zn^{2+}	31.97	0.21	12.04	24.68	117.5

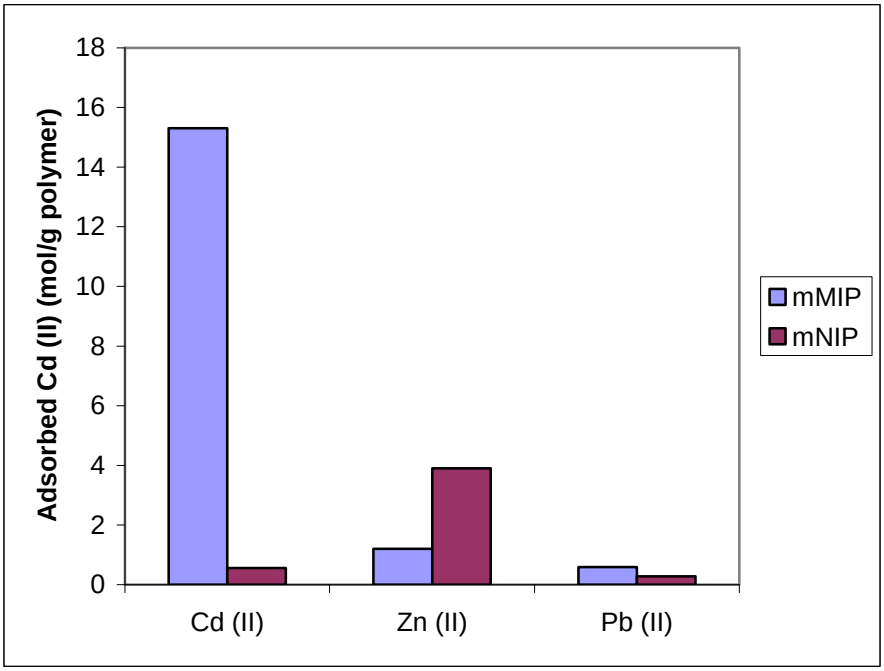

Figure 3.16. Adsorbed template and competitive ions both in mMIP and mNIP beads. Vtotal: 10 mL, 10 mg/L solution, 25 mg polymer and T: 25^{o}C.

3.5 Adsorption of Cd^{2+} from human plasma with MSFB system

3.4.1 Effect of Time

The continue-wise adsorption tests of Cd^{2+} ions from human plasma were studied for the mMIP and mNIP beads. Figure 3.17 shows the time dependence of the adsorption values of Cd^{2+} ions on Cd^{2+} imprinted magnetic poly(HEMA-MAC) beads. The adsorption rate was relatively very fast, the time required to reach equilibrium conditions was about 30 min. The maximum adsorption capacity for Cd^{2+} ions was 46.85 μmol per gram dry weight of beads. This fast adsorption

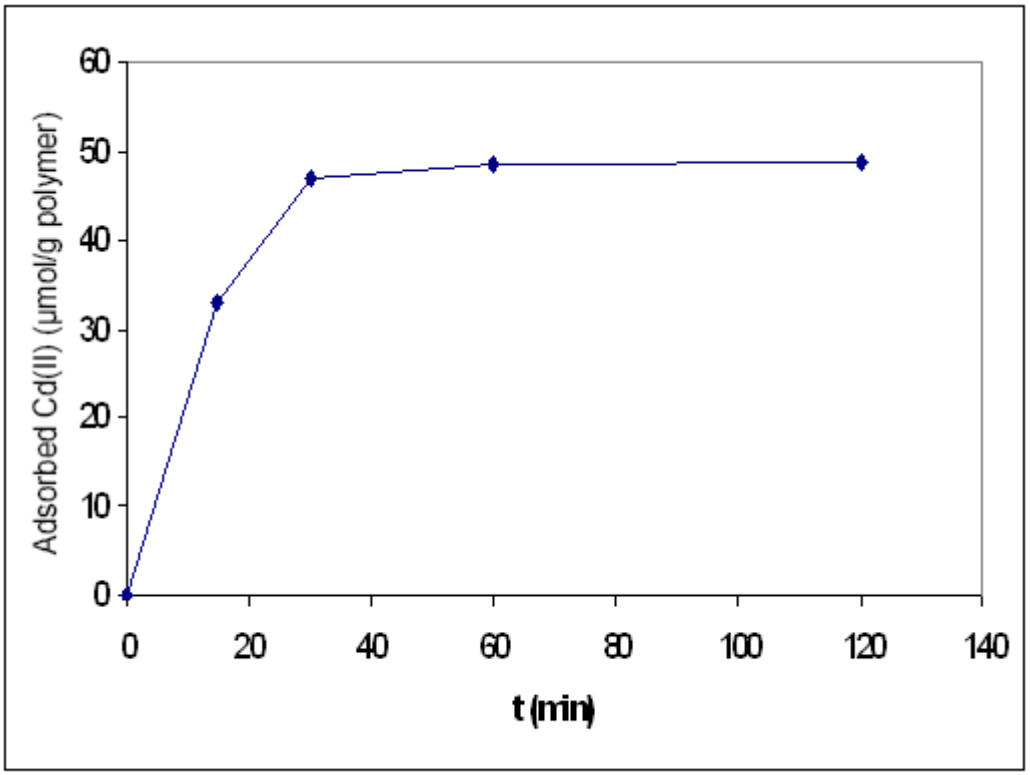

Figure 3.17 Time dependent adsorption of Cd^{2+} ions on the Cd^{2+}-imprinted magnetic poly(HEMA- MAC) beads, Initial concentrarion of metal ions: 40 mg l^{-1}; *T*: 25°C.

equilibrium is most probably due to high complexation and geometric affinity between Cd^{2+} ions and Cd^{2+} cavities in the beads structure.

3.5.2 Effect of Initial Concentration of Cd^{2+} ions

Figure 3.18 shows the equilibrium concentration of metal ions dependence of the adsorbed amount of the Cd^{2+} onto mMIP beads. The adsorption values increased with increasing concentration of Cd^{2+} ions, and a saturation value is achieved at ion concentration of 40 mg/L as 48.8 μmol/g polymer as maximum adsorption capacity, which represents saturation of the active binding cavities on the mMIP beads.

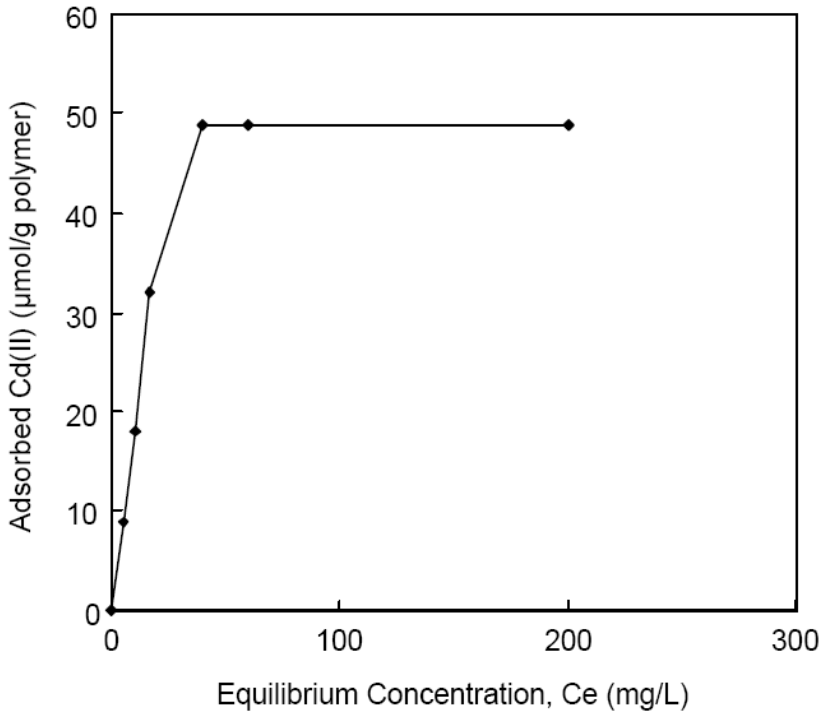

Fiure 3.18 Adsorption isotherm of mMIP beads: Flow rate: 0.5 ml/min; T: 25oC.

3.5.3 Langmuir Adsorption Model

During the MSFB "experiments, adsorption isotherms were used to evaluate adsorption properties. The Langmuir adsorption isotherm is expressed by Equation 4.3. The corresponding transformations of the equilibrium data for Cd^{2+} ions gave rise to a linear plot, indicating that the Langmuir model could be applied in these systems and described by the equation:

$$Q = Q_{max}. b . C_{eq}/ (1+bC_{eq}) \qquad (3.9)$$

where Q is the concentration of bound Cd^{2+} ions in the adsorbent (µmol/g), Ceq is the equilibrium Cd^{2+} ions concentration in solution (µmol /L), b is the Langmuir constant (g/µmol) and, Q_{max} is the adsorption capacity (µmol/g). This equation can be linearized so that

$$1/Q = [1/(Q_{max}. b)][1/C_{eq}] + [1/(Q_{max}.] \qquad (3.10)$$

The plot of $1/C_{eq}$ versus 1/Q was employed to generate the intercept of 1/Qmax and the slope of $1/Q_{max}$.b (Figure 3.19).

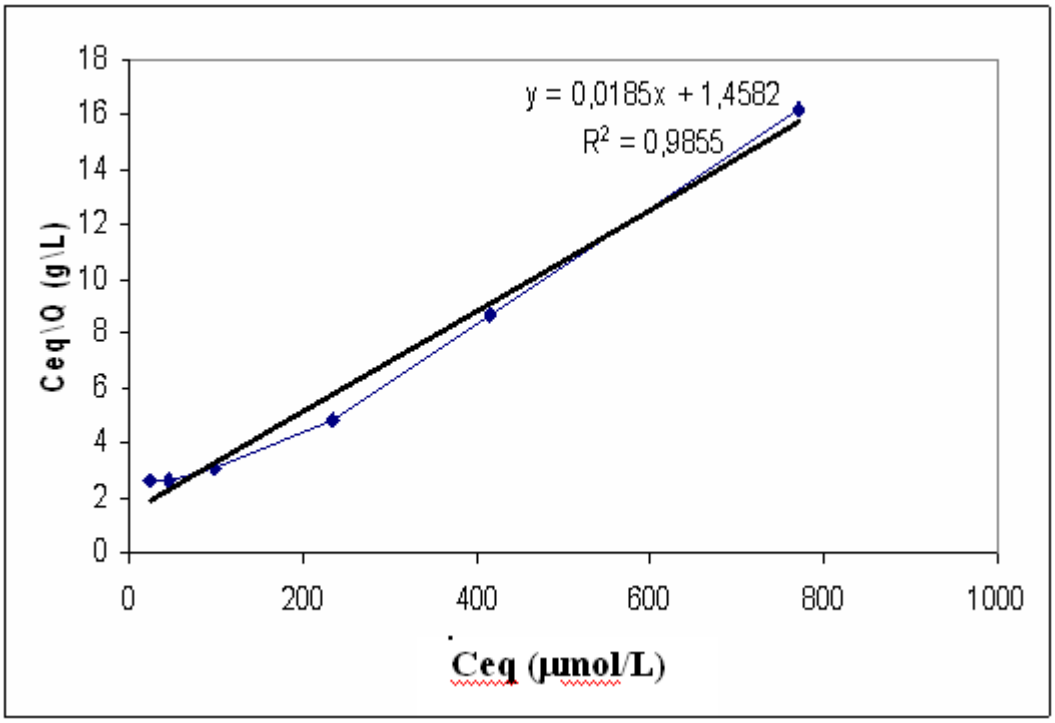

Figure 3.19. Langmuir adsorption isotherm. Cd^{2+} ions concentration 40 mg/L; pH: 7.4; T: 25°C.

The maximum adsorption capacity (Q_{max}) data for the adsorption of Cd^{2+} ions was obtained from the experimental data. The correlation coefficients (R^2) were 0.98 at pH 7.4. The Langmuir adsorption model can be applied in this affinity adsorbent system. It should be also noted that the maximum adsorption capacities (Q_{max}) and the Langmuir constants were found to be 54.05 μmol/g (pH 7.4) and 1.26 10^{-2} g/μmol, respectively. In order to examine the controlling mechanism of adsorption process such as mass transfer and chemical reaction, kinetic models were used to test experimental data. The kinetic models (Pseudo-first and second-order equations) can be used in this case assuming that the measured concentrations are equal to adsorbent surface concentrations. The first-order rate equation of Lagergren is one of the most widely used for the adsorption of solute from a liquid solution (Cheung et al., 2001). It may be represented as follows:

$$\Delta q_t/dt=k_1(q_{eq}-q_t) \quad (3.11)$$

where k_1 is the rate constant of pseudo-first order adsorption (min^{-1}) and q_{eq} and q_t denote the amounts of adsorbed protein at equilibrium and at time t (mg/g), respectively. After integration by appliying boundary conditions, $q_t=0$ at t=0 and $q_t=q_t$ at t=t, gives

$$\log[q_{eq}/(q_{eq}-q_t)]=(k_1t)/2.303 \quad (3.12)$$

Equation 4.6 can be rearranged to obtain a linear form

$$\log(q_{eq}-q_t)=\log(q_{eq})-(k_1t)/2.303 \quad (3.13)$$

a plot of $\log(q_{eq})$ versus t should give a straight line to confirm the applicability of the kinetic model. In a true first-order process $\log q_{eq}$ should be equal to the interception point of a plot of $\log(q_{eq}-q_t)$ via t.

In addition, a pseudo-second order equation based on adsorption equilibrium capacity may be expressed in the form,

$$\Delta q_t/dt=k_2(q_{eq}-q_t)^2 \quad (3.14)$$

Where k_2 (g mg^{-1} min^{-1}) is the rate constant of pseudo-first order adsorption process. Integrating equation 4.8, q and applying the boundary conditions, $q_t=0$ at t=0 and $q_t=q_t$ at t=t, leads to

$$1/(q_{eq}-q_t)]=(1/q_{eq})+k_2t \quad (3.15)$$

or equivalently for linear form

$$(t/q_t)=(1/k_2q_{eq}^2)+(1/q_{eq})t \quad (3.16)$$

a plot of t/q_t versus t should give a linear relationship for the applicability of the second-order kinetics. The rate constant (k_2) and adsorption at equilibrium (q_{eq}) can be obtained from the intercept and slope, respectively.

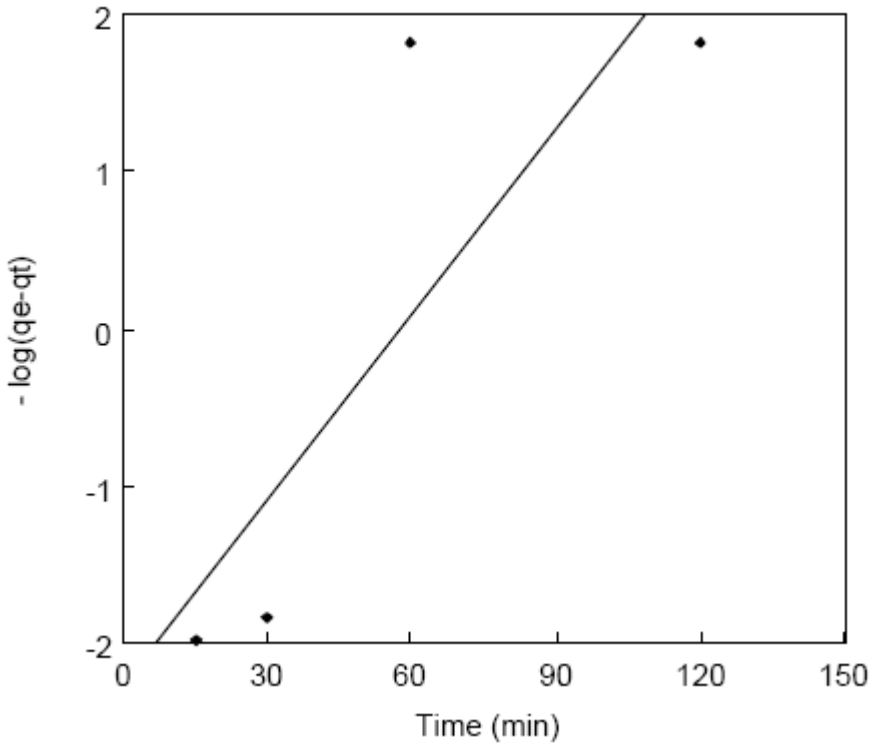

Figure 3.20. Pseudo-first-order kinetic of the experimental data for the adsorbent.

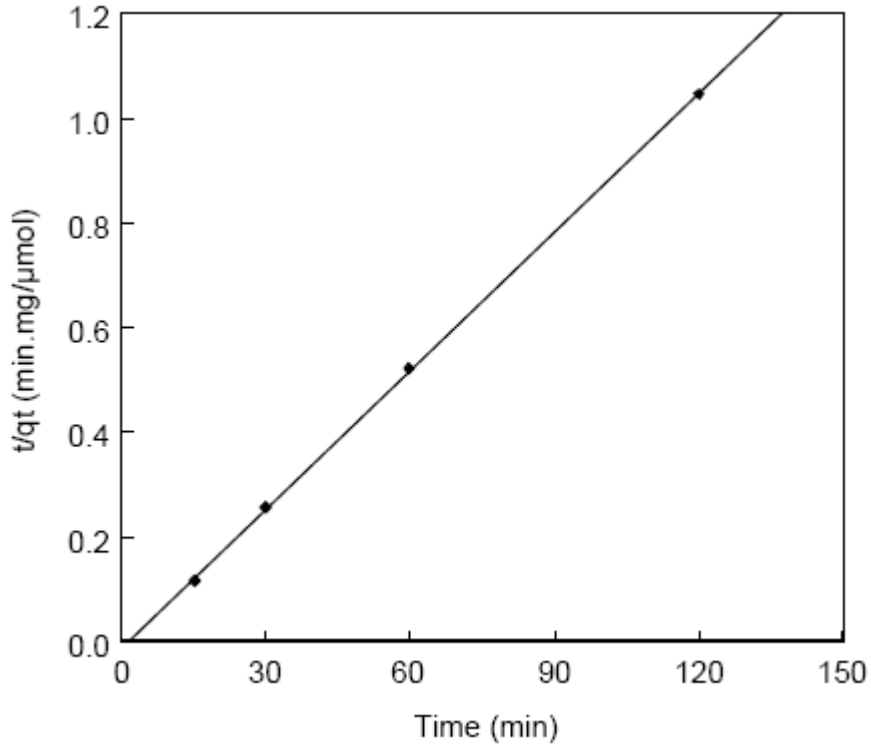

Figure 3.21. Pseudo-second-order kinetic of the experimental data for the adsorbent.

Table 3.4 Kinetic constants for the mMIP beads.

Initial Conc. (mg/L)	**Experimen.**	**First-order kinetic**			**Second-order kinetic**		
		slope	*intercept*		*intercept*	*slope*	
	Qeq (μmol/g)	k_1 (1/min)	q_{eq} (μmol/g)	R^2	k_2 (g/μmol)	q_{eq} (1/min)	R^2
40	48.8	2.76 x 10-^{3}	86.55	0.45	6.45 x 10^{-3}	113.63	0.99

Table 3.5 Langmuir and Freundlich adsorption isotherm constants.

	Experimental	Langmuir model			Freundlich model		
	Qexp (μmol/g)	Qmax (μmol/g)	b	R^2	K_F	n	R^2
mNIP	4.2	5.9	2.96.10^{-3}	0.95	63.37	1.66	0.91
mMIP	48.8	54.1	1.26.10^{-2}	0.98	2.58	0.49	0.85

3.5.4 Selectivity Experiments

Adsorption capaties of the Cd^{2+}-imprinted magnetic poly(HEMA-MAC) beads for metal ions under competitive conditions (i.e. adsorption from solutions containing 10 mg/l from each of Cd (II), Zn(II) adn Pb(II) ions) are given Table 4.2. Table 3.6 summarizes K_d, and k, values of Pb^{2+} and Zn^{2+} with respect to Cd^{2+}.

Table 3.6. K_d (ml/g), k, and values of Pb^{2+} and Zn^{2+} with respect to Cd^{2+}.

Metal Ion	mNIP Beads		mMIP Beads		k'
	K_d	k	K_d	k	
Cd^{2+}	6.50	-	301.7	-	
Pb^{2+}	6.09	1.06	12.8	23.6	22.6
Zn^{2+}	27.40	0.23	8.2	37.0	160.7

* Metal ion concentration: 40 mg/L for all metal ions.

3.5.5. Effect of flow-rate

Adsorption capacity of Cd^{2+} ions of the MIP at different flow rates is shown in Figure 3.22. Cd^{2+} adsorption capacity decreased drastically from 48.8 µmol/g to 20.0 µmol/g with increase of the flow rate from 0.50 ml/min to 3.0 ml/min. When the flow rate decreases contact time in the column is longer. Thus, Cd^{2+} ions have more time to diffuse to the pores mMIP beads and to bind to the Cd^{2+} molecular cavities, hence a better adsorption capacity obtained. In addition, for column operation the mMIP beads are continuously in contact with fresh human plasma. Consequently the concentration in the plasma in contact with a given layer of beads in a column is relatively constant. For batch treatment, the concentration solute in contact with a specific quantity of adsorbent steadily decreases as adsorption proceeds, thereby decreasing the effectiveness of the adsorbent for removing the solute.

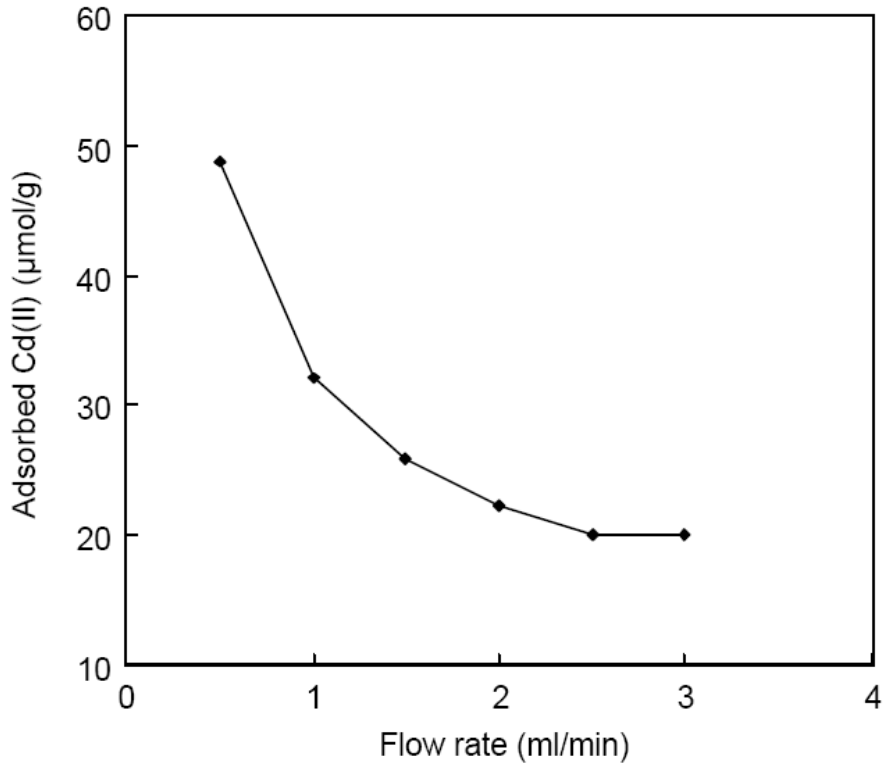

Figure 3.22 Effect of flow rate on Cd^{2+} adsorption. Cd^{2+}: 40 mg/L, 25 ^{o} C

3.5.6 Desorption and Repeated Use

The regeneration is one of the most important strongpoint of MIPs, with this capability of MIPs being considered as having a great influence on their extended application in improving process economics. For this reason, the regeneration porperty of mMIP beads is worthy of study. Desorption of the Cd^{2+} ions from the mMIP beads was performed. Various factors are probably involved in determining rates of Cd^{2+} desorption, such as the extent of hydration of the metal ions and polymer microstructure. However, an important factor appears to be binding strength. In this study, the desorption time was found to be 30 min. Desorption ratios are high (up to 95%). In order to obtain the reusability of the mMIP beads, adsorption-desorption cycles were repeated 10 times using the same mMIP beads. The adsorption capacity of the recyled mMIP beads can still be maintained at 97% level at the 10th cycle (Figure 3.23). It can be concluded that the mMIP beads can be used many times without decreasing their adsorption capacities significantly.

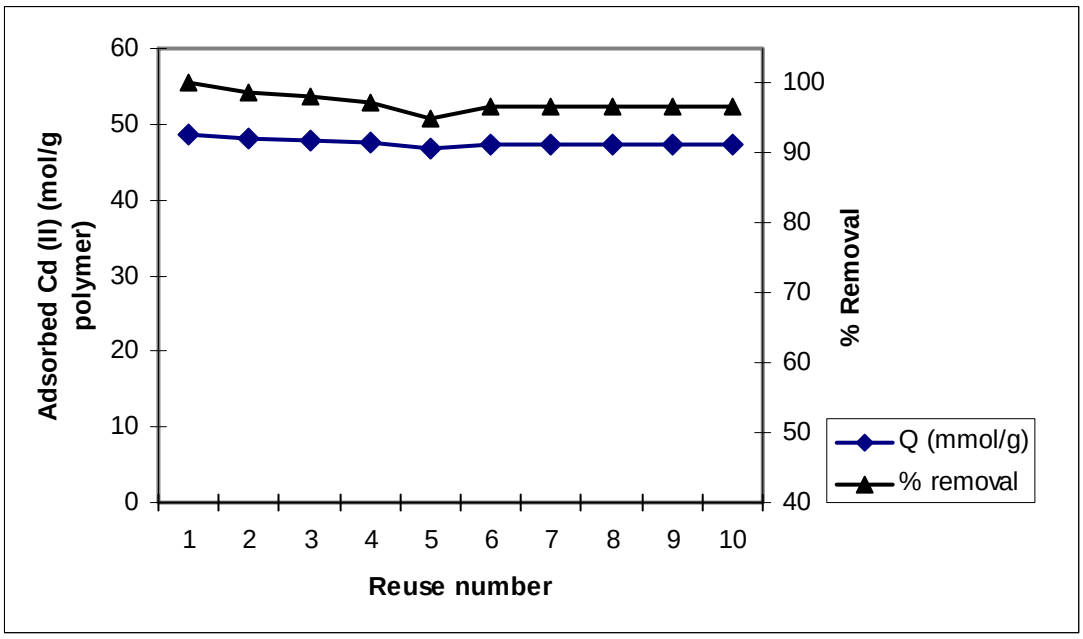

Figure 3.23. Adsorption-Deaorption Cycle of Cd^{2+}-imprinted magnetic poly(HEMA-MAC) beads; pH: 7.4. T: 25°C.

As seen Fig. 3.23, the removal percent of Cd^{2+} ions is not significantly changed with increasing reuse number.

In conclusion, we prepared Cd^{2+} imprinted non-magnetic beads (in the size range of 63-140 μm in diameter) by suspension polymerization (Andaç et al., 2004). Adsorption chromatography with a packed column of beads as a support material is not easy to scale up because the pressure drop in packed columns is high, leading to compaction of the bed under pressure and low flow rates (Benes et al., 2005). Rigid porous beads overcome the compressibility problem, but the bead size employed to prevent high operating pressures may lead to diffusional limitations which degrade performance. Packed-bed columns usually require long elution times. The development of alternative methods is therefore of considerable interest. Magnetically stabilized fluidized bed enables the use of magnetic processing for rapid and selective removal. Especially, when dealing with highly viscous mediums such as blood contact with the magnetic adsorbent in a magnetically stabilized fluidized bed is desirable because of high convective transport rates without cell damage (i.e., hemolysis). This results in a rapid processing, which greatly improves the adsorption, washing, desorption and regeneration steps and decreases the probability of inactivation of biomolecules**.** In this study, the relative selectivity coefficient is an indicator to express an adsorption affinity of recognition sites to the imprinted Cd^{2+} ions. The results showed that the mMIP beads for Cd^{2+} / Pb^{2+} and Cd^{2+} / Zn^{2+} were 22.6 and 160.7 times greater than mNIP matrix, respectively. The mMIP beads can be used many times without decreasing their adsorption capacities significantly.

REFERENCES

Albert, R.V. & Tien, C. (1985). Particle collection in magnetically stabilized fluidized filters. *American Institute of Chemical Engineers Journal*s, *31,* (2), 288-297.

Andaç, M., Say R. & Denizli A. (2004). Molecular recognition based cadmium removal from human plasma. *Journal of Chromatography B, 811,* 119-126.

Arshady, R. & Mosbach, K. (1981). Synthesis of substrate-selective polymers by host-guest polymerization. *Makromol. Chem., 182,* 687–692.

Asokan, P., Dixit, R., Mukhtar, H., & Murti, C.R.K. (1981). Effect of cadmium on hepatic mixed function oxidases during the early development of rats; possible protective role of metallothionein. *Biochemistry Pharmacology, 30* (22), 3095-3098.

Benes M.J., Horak D., Svec F. (2005) Methacrylate-based chromatographic media. Journal of Separation Science, *28* 1855-1875.

Broughton, D. B. & Gembicki, S. A. (1984). Production-scale adsorptive separations of liquid mixtures. *AIChE Symp. Ser*, 80, (233), 62-67.

Buchet, J.P., Roels, H., Lauwerys, R., Vandevoorde, A., & Pycke, J.M. (1983). Oral daily intake of cadmium, lead, manganese, copper, chromium, mercury, calcium, zinc, and arsenic in Belgium: a duplicate meal study. *Food chem. Toxicol., 21,* 19-24.

Burns, M. A. & Graves, D. J. (1985). Continuous affinity chromatography using a. magnetically stabilized fluidized bed. *Biotechnology Progress, 1,* (2), 95-103.

Carlton-Smith, C.H. (1987). Effects of metals in sludge-treated soils on crops, Medmenham, United Kingdom, Water Research Centre (Environment TR/251).

Cheung, C.W., Porter, J.F., Mckay, G., (2001), Sorption kinetic analysis for the removal of cadmium ions from effluents using bone char.Water Research, 605-612.

Davis, R.D. & Coker, E.G. (1980) Cadmium in agriculture, with special reference to the utilisation of sewage sludge on land, Medmenham, United Kingdom, Water Research Centre (Technical Report TR/139)

Decker, L.E., Byerrum, R.U., Decker, C.F., Heppert, C.A., & Langham, R.F. (1958). Chronic toxicity studies. I. Cadmium administered in drinking-water to rats. *Am. Med. Assoc. Arch.Ind. Health, 18*, 228-231.

Denizli, A., Tanyolaç, D., Salih B., & Özdural, A. (1998). Cibacron Blue F3GA-attached polyvinylbutyral microbeads as novel magnetic sorbents for removal of Cu(II), Cd(II) and Pb(II) ions. *Journal of Chromatography A, 793,* 47-56.

Duce, R.A., Hoffman, G.L., & Zeller, W.H. (1975). Atmospheric trace metals at remote northern and southern hemisphere sites: pollution or natural. *Science, 187*, 59-61.

Duce, R.A., Arimoto, R., Ray, B.J., Unni, C.K., & Harder, P.J. (1983). Atmospheric trace elements at Enewetok Atoll. I. Concentration, sources, and temporal variability. *J. Geophys. Res. 88,* 5321-5342.

Elinder, C.-G., Kjellström, T., Lind, B., Linnman, L., Piscator, M., & Sundstedt, K. (1983). Cadmium exposure from smoking cigarettes: variations with time and country where purchased. *Environmental Research 32*, 220-227.

Elinder, C.-G., Kjellström, T., Lind, B., & Linnman, L. (1976). Cadmium concentration in kidney cortex, liver, and pancreas among autopsied Swedes. *Arch. environ. Health, 31,* 292-302.

Elinder, C.-G., Kjellström, T., Linnman, L., & Pershagen, G. (1978) Urinary excretion of cadmium and zinc among persons from Sweden. *Environmental Research 15*: 473-484.

Elinder, C.-G. & Piscator, M. (1978). Cadmium and zinc in horses. In: Kirchgessner, M., ed. Proceedings of the 3rd International Conference on Trace Elements in Man and Animals, Freising-Weihenstephan, Federal Republic of Germany, 25-29 July, 1977, Freising-Weihenstephan, Munich Technical University,pp. 569-572.

Ensing, K. & De Boer, T. (1999)**.** Molecular imprints and related approaches for solid-phase extraction and sensors in chemical analysis. *Trends in Analytical Chemistry, 18,* 138-145.

Flanagan, P.R., Mclellan, J.S., Haist, J., Cherian, M.G., Chamberlain, M.J., & Valberg, L.S. (1978). Increased dietary cadmium absorption in mice and human subjects with iron deficiency. *Gastroenterology, 74,* 841-846.

Forstner, U. (1980). Cadmium in the environment, Part I. In: Nriagu, J.O., ed. Cadmium in polluted sediments, New York, Chichester, John Wiley & Sons, pp. 305-363.

Frank, A., Peterson, L., & Morner, T. (1981). Lead and cadmium levels in organs from moose, deer, and hare. *Svensk Veterinaertid., 33,* 151-156 (in Swedish).

Friberg, L., Piscator, M., Nordberg, G., & Kjellström, T. (1974). Cadmium in the environment, 2nd ed., Cleveland, Ohio, CRC Press, pp. 248.

Friberg, L., Elinder C.G. & Kjellström T. (1992). Cadmium, Environmentel Health Criteria ISBN 92 4 157134 9, University of Aucland, New Zealand, pp. 280.

Greenberg, R.R., Gordon, G.E., Zoller, W.H., Jacko, R.B., Nevendorf, D.W., & Yost, K.J. (1978). Composition of particles emitted from the Nocosia municipal incinerator. *Environmental Science Technology, 12*, (12), 1329-1332.

Hagino, N. & Yoshioka, K. (1961). A study on the etiology of Itai-itai disease. *J. Jpn. Orthop. Assoc.,* 35, 812-815 (in Japanese).

Haupt, K. & Mosbach, K., (1998). Plastic antibodies: developments and applications. *Trends Biotechnology, 15,* (11) 468– 475.

Heindryckx, R., Demuynck, M., Dams, R., Janssens, M., & Rahn, K.A. (1974). Mercury and cadmium in Belgian aerosols. In: Problems of the contamination of man and his environment by mercury and cadmium. CEC European Colloquium, July, 1973, Luxembourg, Commission of the European Communities, pp. 135-148.

Huang, S.H., Liao, M.H., Chen, D.H. (2003) *Biotechnology Progress 19,* 1095-1099

Janssens, M. & Dams, R. (1974). Determination of cadmium in air particulates by flameless atomic absorption spectrometry with a graphite tube. *Analytical Chimica Acta*, *70,* 25-33.

Japanese Envıronment Agency (1974). Results of measurement at the national air sampling network stations, Tokyo, Japanese Environment Agency, Air Pollution Control Division, Air Quality Bureau, pp. 159 (in Japanese).

Järup, L., Rogenfelt, A., Elinder, C.-G., Nogawa, K., & Kjellström, T. (1983). Biological half-time of cadmium in the blood of workers after cessation of exposure. Scand. J. *Work Environmental Health, 9,* 327-331.

Jeffery, E.H., Noseworthy, R., & Cherian, M.G. (1989). Age dependent changes in metallothionein and accumulation of cadmium in horses. *Comparative Biochemistry Physiology* 93C, 327-332.

Jones, D. T. (1974). *Process Biochemistry, 9,* (12), 17-19.

Just, J. & Kelus, J. (1971). Cadmium in the air atmosphere of ten selected cities in Poland. *Rocz. Panstw. Zakl. Hig*., *22*, 249-256 (in Polish).

Keller, G.E. (1983) Gas adsorption processes: State of the art, *Industrial Gas Separations*. In: T.E. Whyte Jr., C.M. Yon and E.H. Wagner, Editors, *ACS Symp. Ser. 223*, American Chemical Society, Washington D.C. (1983), pp. 145–169.

Kjellström, T., Elinder, C.-G., & Friberg, L. (1984). Conceptual problems in establishing the critical concentration of cadmium in human kidney cortex. Environ*mental Research*, *33*, 284-295.

Kjellström, T., Frıberg, L., & Rahnster, D. (1979) Mortality and cancer morbidity among cadmium-exposed workers. *Environmental Health Perspect., 28* 199-204.

Kneip, T.J., Eisenbud, M., Strehlow, C.D., & Freudenthal, P.C. (1970) Airborne particulates in New York City. *J. Air Pollution Control Associate, 20,* 144-149.

Kriz, D., Ramstrom, & O., Mosbach, K. (1997). Molecular. imprinting-new possibilities for sensor technology. *Analytical Chemistry, 69,* 345–349.

Lee, W. K. (1983) *AIChE Symp. Ser*., *222,* (79), 87-96.

Lauwerys, R., Buchet, J.P., & Roels, H. (1975). Effets subcliniques de l'exposition humaine au cadmium. In: Proceedings of the International Symposium on Problems of the Contamination of Man and His Environment by Mercury and Cadmium, Luxembourg, Commission of the European Communities, pp. 447-461.

Lauwerys, R., Roels, H., Regnıers, M., Buchet, J.P., Bernard, A., & Goret, A. (1979). Significance of cadmium concentration in blood and in urine in workers exposed to cadmium. *Environmental Research*, 20, 375-391.

Lucas, P.A., Jarivalla, A.G., Jones, J.H., Gough, J., & Vale, P.T. (1980). Total cadmium fume inhalation. *Lancet*, *2,* (8187), 205.

Lund, L.J., Betty, E.E., Page, A.L., & Elliott, R.A. (1981). Occurrence of naturally high cadmium levels in soils and its accumulation by vegetation. *Journal Environmental Quality,* 10, 551-556.

Margoshes, M. & Vallee, B.L. (1957). A cadmium kidney protein from equine kidney cortex. *J. Am. Chem. Soc., 79,* 4813-4814.

Martin, J.H. & Broenkow, W.W. (1975) Cadmium in plankton: elevated concentrations of Baja California. *Science, 190*, 884-885.

Mclellan, J.S., Flanagan, P.R., Chamberlain, M.J., & Valberg, L.S. (1978). Measurements of dietary cadmium absorption in humans. *Journal Toxicology Environmental Health*, 4, 131-138.

Mosbach, K., & Ramström, O. (1996). The emerging technique of molecular imprinting and its future impact on biotechnology, *Bio/Technology,* 14, 163–170.

Mosbach, K., Haupt, K., Liu, X.-C., Cormack, & P.A.G., Ramström, O. (1998). in: Bartsch, R.A., Maeda, M. (Eds.), Molecular and Ionic Recognition with Imprinted Polymers, ACS Symposium Series, Vol. 703.

Mosbach, K., & Cormack, P. (1999). Molecular imprinting: recent developments and the road ahead, *Reactive & Functional Polymers, 41,* 115–124.

Mosbach, K., Ye, L., & Cormack, P. (2001). Molecular imprinting on microgel spheres, *Analytica Chimica Acta, 435,* 187–196.

Neeb, R. & Wahdat, F. (1974). About inverse voltammetry analysis of cadmium in aerosols. *Z. Analytical Chemistry, 269,* 275-279 (in German).

Nielsen, S.A. (1975). Cadmium in New Zealand dredge oysters, geographic distribution. *International Journal Environmental Analytical Chemistry*, 4, 1-7.

Nriagu, J.O. (1979). Global inventory of natural and anthropogenic emissions of trace metals to the atmosphere. *Nature (Lond.), 279,* 409.

Nordberg, G.F., Goyer, R.A., & Nordberg, M. (1975). Comparative toxicity of cadmium metallothionein and cadmium chloride on Mouse kidney. *Archieve Pathology,* 99, 192-197.

Nordberg, M. (1978). Studies on metallothionein and cadmium. *Environmental Research, 15,* 381-404.

Nordberg, M. (1984). General aspects of cadmium transport, uptake, and metabolism by the kidney. *Environmental Health Perspect, 54,* 13-20.

Nordberg, G.F., Slorach, S., & Stenstrom, T. (1973) Cadmium poisoning caused by a cooled soft drink machine. *Läkartidningen*, 70: 601-604 (in Swedish with English summary).

Nogawa, K., Tsuritani, I., Kido, T., Honda, R., Yamada, Y., & Ishizaki, M. (1987). Mechanism for bone disease found in inhabitants environmentally exposed to cadmium: decreased serum 1alpha,25-dihydroxyvitamin D level. *Int. Arch. Occup. Environmental Health, 59,* 21-30.

Özkara, S., Akgöl, S., Çanak, Y., Denizli, A. (2004) A novel magnetic adsorbent for immunoglobulin-G purification in a magnetically stabilized fluidized bed. *Biotechnology Progress* 20 (4),1169-1175.

Piscator, M. (1964). On cadmium in normal kidneys together with a report on the isolation of metallothionein from livers of cadmium-exposed rabbits. *Nord. Hyg. Tidskr*., 45, 76-82 (in Swedish).

Page, A.L., Bıngham, F.T., & Shang, A.C. (1981). Cadmium. In: Lepp, N.W., ed. Effect of heavy metal pollution on plants, Barking, Essex, Applied Science Publishers, Vol. 1, pp. 77-109.

Piletsky, SA., Panasyuk, TL., Piletskaya, EV., Nicholls, IA., & Ulbricht, M., (1999). Receptor and transport properties of imprinted polymer membranes – a review, *J. Membr. Sci*., 157, 263–278.

Rahola, T., Aaran, R.-K., & Miettinen, J.K. (1972). Half-time studies of mercury and cadmium by whole-body counting. In: Assessment of radioactive contamination in man, New York, International Atomic Energy Agency Unipublishers, pp. 553-562 (IAEA Proceedings Series No. Sm-150/13).

Robbins, S.L., Cotran, R.S., & Kumar, U. (1984). Pathological basis of disease, 3rd ed., Philadelphia, Pennsylvania, W.B. Saunders & Co., pp. 1327-1328.

Rosenweig, R. E. (1979). The quiescent fluid-like state for the magnetically stabilized fluidized bed (MSB), *Indian Engering Chemistry Fundanmental 18,* 260-269.

Swartz, H.M., Bolton, J.R., Borg, D.C., Bological Applications of Electron Spin Resonance*Bological Applications of Electron Spin Resonance,* Wiley, New York, 1972.

Scherer, G. & Barkemeyer, H. (1983). Cadmium concentrations in tobacco and tobacco smoke. *Ecotoxicol. Environ. Saf., 7,* 71-78.

Shea, KJ., & Dougherty, TK., (1986). Molecular recognition on synthetic amorphous surfaces. The influence of functional group positioning on the effectiveness of molecular recognition, *J. Am. Chem. Soc., 108,* 1091–1093.

Sellergren, B., Andersson, L. (1990). Molecular recognition in macroporous polymers prepared by a substrate analogue imprinting strategy, *J. Org. Chem., 55,* 3381–3383.

Sellergren, B. (1997). Imprinted polymers: stable, reusable antibodymimics for highly selective separations, *Am. Lab., 14,* 163–167.

Shaikh, Z.A. & Smith, J.C. (1980). Metabolism of orally ingested cadmium in humans. In: Holmstedt, B., Lauwerys, R., Mercier, M., & Roberfroid, M., ed. Mechanisms of toxicity and hazard evaluation, Amsterdam, Elsevier/North Holland Biomedical Press, pp. 569-574.

Siegel, J. H. (1982). *Ind. Eng. Chem. Process. Des. Dev.,* 21, 135-141.

Siegel, J. H. (1988). Liquid-fluidized magnetically stabilized beds. *Powder Technol. 52,* 139-148.

Sussman, M. V. (1976). Continuous chromatography. *Chem. Tech., 6,* 260-266.

Tanaka, K. (1982). Effects of hepatic disorders on the fate of cadmium in rats. In: Foulkes, E.C., ed. Biological roles of metallothionein, Amsterdam, Oxford, New York, Elsevier Science Publishers, pp. 237-249.

Tarasenko, N.Yu. & Vorobjeva, R.S. (1973) [Hygienic problems connected with the use of cadmium.] Vestn. Akad. Med. Nauk. SSR, 28: 37-43 (in Russian with English abstract).

Terranova, B., & Burns, M. A., (1989). Removal of Cell Debris using a Magnetically Stabilized Fluidized Bed. ,*Biotechnology Proress, 5,* (3), 98-104.

Tjell, J.C., Hansen, J.A., Christensen T.H., & Hovmand, M.F. (1981). Prediction of cadmium concentrations in Danish soils. In: L'Hermite, P. & Ott, H., ed. Characterization, treatment and use of sewage sludge, Dordrecht, Reidel Publishing Co., pp. 652-664.

Tohyama, C., Shaikh, Z.A., Nogawa, K., Kobayashi, E., & Honda, R. (1981). Elevated urinary excretion of metallothionein due to environmental cadmium exposure. *Toxicology, 22,* 289-297.

Vahter, M., ed. (1982) Assessment of human exposure to lead and cadmium through biological monitoring, Stockholm, National Swedish Institute of Environmental Medicine and Department of Environmental Hygiene, Karolinska Institute, 136 pp (Report prepared for the United Nations Environment Programme and the World Health Organization).

Vlatakis, G., Andersson, L.I., Muller, R., Mosbach, K. (1993). Drug assay using antibody mimics made by molecular imprinting Drug assay using antibody mimics made by molecular imprinting. *Nature, 361,* 645–647.

Wulff, G., & Sarhan, A., (1972), The use of polymers with enzyme analogous structures for the resolution of racemates, *Angew. Chem. Int. Ed. Engl., 11,* 341, (Angew. Chem., 84, 364).

Wulff, G. (1995). Molecular imprinting in cross-linked materials with the aid of molecular templates-a way towards artificial antibodies. *Angew. Chem. Int. Ed. Engl., 34*, 1812–1832.

Wulff, G., Strikovsky, A., & Hradil, J. (2003). Catalytically active, molecularly imprinted polymers in bead form. *Reactive & Functional Polymers*, *54,* 49–61.

Wulff, G., Sarhan, A., & Zabrocki, K. (1973). Enzyme-analogue polymers and their use for the resolution of racemates. *Tetrahedron Letter* , *44,* 4329–4332.

Wulff, G. (1982). Selective binding to polymers via covalent bonds. The construction of chiral cavities as specific receptor sites. *Pure Appl. Chem., 54*, 2093–2102.

Wulff, G., Poll, H-G., & Minarik, M. (1986). Enzyme-analogue built polymers. XIX Racemic resolution on polymers containing chiral cavities, *J. Liq. Chromatogr., 9,* 385–405.

Wilson, D.N. (1988) Cadmium - market trends and influences. In:Cadmium 87. Proceedings of the 6th International Cadmium Conference, London, Cadmium Association, pp. 9-16.

Wolff, E.W. & Peel, D.A. (1985). The record of global pollution in polar snow and ice. Nature (Lond.), 313: 535-540.

Wolnik, K.A., Fricke, F.L., Caper, S.G., Braude, G.L., Meyer, M.W., Satzger, R.D., & Bonnin, E. (1983). Elements in major raw agricultural crops in the United States. I. Cadmium and lead in lettuce, peanuts, potatoes, soybeans, sweet corn, and wheat. *J. Agric. Food Chem., 31,* 1240-1244.

Yoshikawa, M., Izumi, J., Kitao, T., Koya, S., & Sakamoto, S. (1994). Membranes for enantioselective separation: synthesis and characterization, Preprints for the 16th Annual Meeting of the Membrane Society of Japan, A1-1-1.

Yuh-Shan H. (2006) Reviws of second-order models for adsorption systems. *Journal of Hazardous Materials B, 136*, 681-689.

Zhang, T., Liu, F., Chen, W., Wang, J., & Li, K. (2001). Influence of intramolecular hydrogen bond of templates on molecular recognition of MIP. *Analytica Chimica Acta, 450*, 53–61.